TGFβ Triggers miR-143/145 Transfer From Smooth Muscle Cells to Endothelial Cells, Thereby Modulating Vessel Stabilization

Montserrat Climent, Manuela Quintavalle, Michele Miragoli, Ju Chen, Gianluigi Condorelli, Leonardo Elia

Rationale: **The miR-143/145 cluster is highly expressed in smooth muscle cells (SMCs), where it regulates phenotypic switch and vascular homeostasis. Whether it plays a role in neighboring endothelial cells (ECs) is still unknown.**

Objective: **To determine whether SMCs control EC functions through passage of miR-143 and miR-145.**

Methods and Results: **We used cocultures of SMCs and ECs under different conditions, as well as intact vessels to assess the transfer of miR-143 and miR-145 from one cell type to another. Imaging of cocultured cells transduced with fluorescent miRNAs suggested that miRNA transfer involves membrane protrusions known as tunneling nanotubes. Furthermore, we show that miRNA passage is modulated by the transforming growth factor (TGF) β pathway because both a specific transforming growth factor-β (TGFβ) inhibitor (SB431542) and an shRNA against TGFβRII suppressed the passage of miR-143/145 from SMCs to ECs. Moreover, miR-143 and miR-145 modulated angiogenesis by reducing the proliferation index of ECs and their capacity to form vessel-like structures when cultured on matrigel. We also identified hexokinase II (*HKII*) and integrin β 8 (*ITGβ8*)—2 genes essential for the angiogenic potential of ECs—as targets of miR-143 and miR-145, respectively. The inhibition of these genes modulated EC phenotype, similarly to miR-143 and miR-145 overexpression in ECs. These findings were confirmed by ex vivo and in vivo approaches, in which it was shown that TGFβ and vessel stress, respectively, triggered miR-143/145 transfer from SMCs to ECs.**

Conclusions: **Our results demonstrate that miR-143 and miR-145 act as communication molecules between SMCs and ECs to modulate the angiogenic and vessel stabilization properties of ECs. (*Circ Res*. 2015;116:1753-1764. DOI: 10.1161/CIRCRESAHA.116.305178.)**

Key Words: angiogenesis effect ■ endothelial cells ■ microRNAs ■ smooth muscle myocytes

Vascular endothelium plays a fundamental role in modulating vessel biology and homeostasis.[1] Alteration of its function can induce the development of vessel pathologies, such as atherosclerosis.[2] Several events are involved in angiogenesis, including endothelial cell (EC) division, selective degradation of the basement membrane and the surrounding extracellular matrix, EC migration, and the formation of neovessels.[3] Similar events take place during embryogenesis, but in this context blood vessels are generated from the differentiation of EC precursors, the angioblasts, which associate to form primitive vessels in a process referred to as vasculogenesis.[3] In both cases, once blood vessels are generated, ECs undergo tissue-specific changes creating vessels functionally distinct from each other.[4]

Editorial, see p 1726
In This Issue, see p 1725

The endothelium maturation process is guided also by signals from other cell types. Indeed, development of a vessel's architecture involves the strict association between ECs and mural cells (pericytes and smooth muscle cells [SMCs]): under physiological conditions, communication between these cell types leads to the maturation and stabilization of the vessel.[5,6] These processes involve the action of different growth factors as well as a variety of heterotypic cellular interactions and they could be important mechanisms, by which also pathological signals are transferred from one cell type to another.

MicroRNAs (miRNAs, miRs) constitute a group of short, noncoding RNAs that direct inhibitory complexes to targeted mRNAs.[7] MiRNAs have been implicated in a wide variety of physiological and pathological processes, including those of vessels.[8–11] Recent studies have revealed that miRNAs are released by cells and exert these effects by modulating processes in

Original received December 9, 2014; revision received March 20, 2015; accepted March 23, 2015. In February 2015, the average time from submission to first decision for all original research papers submitted to *Circulation Research* was 13.9 days.

From IRCCS MultiMedica, Milan, Italy (M.C.); Humanitas Clinical and Research Center, Rozzano (MI), Italy (M.Q., M.M., G.C., L.E.); Milan Unit of the Institute of Genetic and Biomedical Research, Rozzano (MI), Italy (G.C., L.E.); Department of Cardiovascular Diseases, University of Milan, Rozzano (MI), Italy (G.C.); Department of Clinical and Experimental Medicine, Center of Excellence for Toxicological Research (CERT), University of Parma, Parma, Italy (M.M.); and Department of Medicine, University of California, San Diego (J.C.).

The online-only Data Supplement is available with this article at http://circres.ahajournals.org/lookup/suppl/doi:10.1161/CIRCRESAHA.116.305178/-/DC1.

Correspondence to Gianluigi Condorelli, MD, PhD, or Leonardo Elia, PhD, Via Manzoni 113, 20089 Rozzano (MI), Italy. E-mail gianluigi.condorelli@humanitasresearch.it or leonardo.elia@yahoo.com

Nonstandard Abbreviations and Acronyms	
EC	endothelial cell
FBS	fetal bovine serum
MiR	microRNA
SMC	smooth muscle cell
TGF	transforming growth factor
TNTs	tunneling nanotubes
WT	wild-type

recipient cells.[12–14] Thus, miRNAs have intercellular signal transduction capabilities.

MiR-143 and miR-145 are clustered, intergenic miRNAs located on chromosome 5 in humans and chromosome 18 in mice and rats. Other groups,[15–17] as well as ours,[8,10,18] have described the role of these miRNAs in the regulation of vascular homeostasis. In particular, we have demonstrated a critical role of the miR-143/145 cluster in SMC differentiation and vascular pathogenesis. A role for this miRNA cluster has also been suggested in ECs: in response to altered blood flow, their expression was shown to be induced through the upregulation of the KLF2 (Kruppel-like factor) transcription factor with a subsequent transfer to SMCs through EC-released exosomes.[14] Kohlstedt et al[19] then showed the involvement of the AMP-activated protein kinase-p53 pathway in miR-143/145 maturation; miR-143 and miR-145 modulate EC response to shear stress, controlling their common target angiotensin-converting enzyme.

In this study, we demonstrate that SMCs communicate with ECs via miR-143 and miR-145. In particular, cell-to-cell EC/SMC contact induces the activation of miR-143/145 transcription in SMCs, and promotes the transfer of these miRNAs to ECs. Once within ECs, the miRNAs blunt the angiogenic potential of ECs. These findings indicate that the miR-143/145 cluster plays a fundamental role for EC/SMC interaction, modulating EC function and then vascular homeostasis.

Methods

Primary Mouse SMC Isolation and Culture

Aortas from euthanized mice were isolated, washed, cleaned of adventitia in phosphate-buffered saline, and then digested with 1 mg/mL of collagenase (Worthington) and 1 mg/mL of dispase II (Worthington) in 1× Hanks' balanced salt solution at 37°C for 1 hour. The reaction was stopped with DMEM supplemented with 10% fetal bovine serum (FBS), and cells centrifuged for 10 minutes at 1200 rpm. Pellets were resuspended in DMEM (Lonza) supplemented with 10% FBS (Lonza), 2 mmol/L glutamine, 1 mmol/L sodium pyruvate, and 100 U/mL penicillin-streptomycin, and plated in 1% gelatin precoated plates. Primary cells from passages 3 to 6 were used for the experiments. Wild-type (WT) and knockout (KO) cells were isolated from 8-week-old WT and miR-143/145 KO mice.[8]

Scanning Ion Conductance Microscopy

Scanning ion conductance microscopy setup and its working in hopping mode has been previously described.[20,21] Briefly, a piezo-controller (ICnano Scanner Controller, Ionscope Ltd) controlled the 3-axis (*x*, *y*, and *z*) piezo translation stage (Physik Instruments, Germany) with 100-μm closed-loop travel range in *x* and *y*, and 50 μm in the *z* direction. The piezo-stage was driven by a high-voltage amplifier (Physik Instruments, Germany) connected to an ICnano scanner controller. The pipette electrode headstage was connected to a Multiclamp 700B (Molecular Devices). The scan head was placed onto an electric micromanipulator (Scientifica, United Kingdom) based on a motorized platform (Scientifica). Preparations were imaged with a Nikon TE-i inverted microscope (Nikon Corporation, Japan). Nanopipettes (≈80 MΩ tip-resistance) were pulled from borosilicate glass with outside diameter 1.0 mm and inside diameter 0.50 mm (Intracell, United Kingdom) using a laser puller P-2000 (Sutter Inc). Nanopipettes were filled with the same medium used for the cultures, that is, M200 medium (Life Technologies). Surface topographical images of the 2 cells (100×100 μm, 512×512 pixels) were acquired by scanning ion conductance microscopy at 25°C in the same medium supplemented with 10 μmol/L HEPES (Lonza) to keep CO_2 concentration constant during the loop images acquisition. Acquisition and analysis were performed with a customized software.

For cell identification, SMCs were labeled with Vybrant DiO cell-labeling solution (Life Technologies), following manufacturer's instruction, and then seeded with ECs.

Bioinformatics

Potential miR-143 and miR-145 targets were identified using the following algorithms: miRanda (http://microrna.sanger.ac.uk); TargetScan (http://www.targetscan.org); and PicTar (http://pic-tar.bio.nyu.edu), as previously described.[22]

Mouse Aorta Ex Vivo Isolation and Culture

Aortas from euthanized mice were isolated, washed, and cleaned of the adventitia in phosphate-buffered saline, then cut in 2 and cultured in DMEM, as described above, with 10% FBS for 24 hours. They were then washed with phosphate-buffered saline and serum-starved (DMEM with 0.1% FBS) for 24 hours. After starvation, aortas were treated or not with transforming growth factor-β1 (TGFβ1) for 24 hours (10 ng/mL), and digested with 1 mg/mL of collagenase and 1 mg/mL of dispase II in 1× Hanks' balanced salt solution at 37°C for 1 hour. The reaction was stopped with DMEM 10% FBS, and cells centrifuged 10 minutes at 1200 rpm. Pellets were resuspended in phosphate-buffered saline/0.2% FBS/0.5 mmol/L EDTA, and incubated with anti-CD31 (Pecam1), clone MEC13.3 (Biolegend). Then, anti-rat magnetic beads (Life Technologies) were used to separate the endothelial layer from the SMC layer. After magnetic separation, EC and SMC fractions were analyzed by fluorescence-activated cell sorter, immuno-histochemistry, and quantitative reverse transcription polymerase chain reaction.

Statistical Analysis

Luciferase, RNA, protein, and proliferation values were compared using 2-tailed ANOVA test. A value of $P \leq 0.05$ was considered to be statistically significant.

Results

miR-143 and miR-145 Transfer From SMCs to ECs

We performed coculture experiments with ECs and SMCs under different conditions. First, the 2 cell types were cocultured using an insert system in which a polyethylene terephthalate membrane separated the 2 cell types in a way that made direct contact impossible (Online Figure IA). In this setup, miR-143/145 was not detected in ECs after 24 and 48 hours of coculture, indicating that under basal conditions, no transfer from SMCs to ECs took place (Online Figure IB and data not shown). Then, a coculture experiment was performed in which the 2 cell types were separately seeded on the 2 sides of a polyethylene terephthalate membrane with a porosity of 1.0 μm, which allowed SMC protrusions to be in direct contact with ECs.[23,24] Using this system, we were able to detect miR-143/145 in ECs after 24 hours of coculture (Figure 1A). To determine whether the contact was inducing direct transfer or de novo transcription of miR-143/145 in ECs, we used a hybrid system in which primary human ECs were cultured

together with primary mouse SMCs. Levels of primary and precursor human miR-143/145 in ECs were unchanged, indicating that contact triggered only the transfer of mature miR-143/145 (Figure 1B and data not shown). In contrast, mature miRNAs were almost undetectable in ECs cocultured with miR-143/145-KO SMCs (Figure 1C).

TGFβ Triggers the Transfer of miR-143/145 From SMCs to ECs

In an effort to understand the molecular mechanism underlying the transfer of miR-143/145, we hypothesized that direct contact between SMCs and ECs induced the production of cytokines directly involved in this process. Thus, we measured the level of TNFα, TGFβ, IL-10, IL-6, and VEGF in conditioned medium from ECs cocultured or not with SMCs. We found that direct contact induced ≈20% to 30% increase in some of these cytokines (Figure 2A; Online Figure IIA). Because it is known that TGFβ signaling is critical for vessel stabilization, and its main source of production are ECs activated by contact with SMCs,[6,25] we hypothesized that TGFβ was a critical factor regulating the transfer of miR-143/145 to ECs. As previously shown,[26] we confirmed in our model that TGFβ is able to augment the differentiation status of SMCs by increasing SMC differentiation markers and miR-143/145 levels (Figure 2B and 2C). When EC/SMC cocultures were treated with a specific and widely used TGFβ pathway inhibitor (SB431542),[27–30] we observed a significant reduction in miR-143/145 transfer to ECs (Figure 2D). This result was further confirmed using SMCs transduced with an shRNA against TGFβR2 (Figure 2E). The inhibitor and shRNA activities were evaluated by quantitative polymerase chain reaction, measuring the expression of the SMC–TGFβ readout genes *Serpine1* (*PAI-1*) and *Smad7* (Online Figure IIB and IIC).[31,32]

Tunneling Nanotubes, Not Exosomes, Mediate the Transfer of miR-143/145 From SMCs to ECs

We then sought to determine the mechanism underlying the transfer of miR-143/145 from SMCs to ECs. To this end, we first cultured ECs in conditioned medium from direct cocultures. We found that conditioned medium did not induce changes in the levels of mature miR-143/145 in ECs (Figure 3A). We then assessed whether miRNA transfer was mediated by the release of exosomes. In fact, when SMCs were cultured with ECs, they secreted exosomes containing high levels of miR-143/145: this effect was blunted when SMCs were treated with the exosome inhibitor GW4869 (Online Figure IIIA), and increased when treated with platelet-derived growth factor or fibroblast growth factor (Online Figure IIIB). These results raised the possibility that ECs were able to uptake SMC-derived exosomes. To address this possibility, we used a lentiviral system to generate SMCs expressing the exosome marker CD63 fused to green fluorescent protein (GFP). However, ECs treated with GFP exosomes purified from the conditioned medium of ECs cocultured with these SMCs did not present any GFP signal at confocal microscopy (data not shown); moreover, ECs challenged with exosomes from SMCs treated with platelet-derived growth factor, fibroblast growth factor, or TGFβ did not present any statistically significant modulation of miR-143/145 (Figure 3B). In addition, the exosome inhibitors GW4869, NH_4Cl, and chloroquine did not reduce miRNA transfer (Online Figure IIIC). Together, these results demonstrate that there is no paracrine transfer of the 2 miRNAs after cell-to-cell contact.

We then evaluated whether miRNA transfer was dependent on specialized membrane proteins. In particular, as the role of gap junctions in mediating miRNA transfer has been suggested,[33,34] we tested whether they played a role also in this model. Treating cells with oleic acid or heptanol—2 well-known gap junction uncoupler agents—was not accompanied by miRNA transfer inhibition (Online Figure IIID). In addition, transduction of SMCs with shRNAs targeting connexin 43 (*Cx43*) was not accompanied by a decrease of miRNA transfer (Online Figure IIIE). These results indicated that gap junctions are not implicated in miRNA transfer.

We subsequently hypothesized that tunneling nanotubes (TNTs) were involved in EC/SMC miRNA transfer. TNTs are small plasma-membrane protrusions recently found to be important for cell communication.[35–37] To test this hypothesis, we used a system in which ECs and SMCs were cocultured and then separated using anti-Pecam1 magnetic beads. This approach was used because the inhibition of TNTs with latrunculin A (LatA), which modifies the cytoskeleton, reduces the ability of cells to grow on polyethylene terephthalate

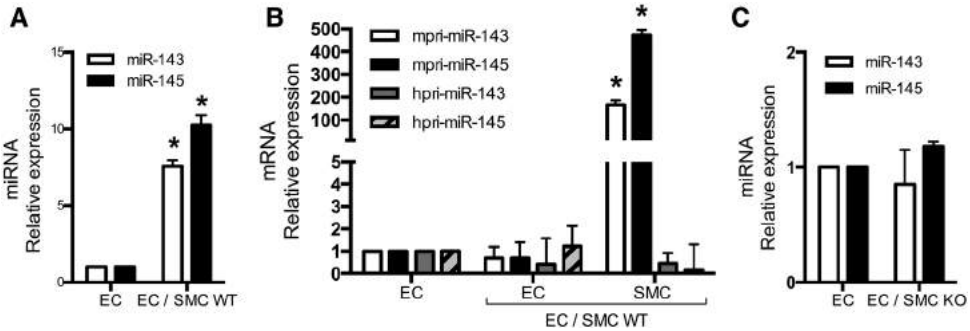

Figure 1. Transfer of miR-143 and miR-145 from smooth muscle cells (SMCs) to endothelial cells (ECs). **A**, Mature miR-143 and miR-145 and (**B**) human and mouse pri-miR-143 and pri-miR-145 were measured in ECs (HUVECs [human umbilical vein endothelial cells]) after culture with wild-type (WT) SMCs. **C**, Mature miR-143 and miR-145 were measured in ECs after 24 hours of coculture with miR-143/145 knockout (KO) SMCs. For quantitative polymerase chain reaction, U6 snRNA was used as internal control. All measurements were calculated as percent of control (EC) and error bars calculated as propagated SEM of triplicate measurements from each experiment. *P<0.05 (each experiment was replicated at least 3×).

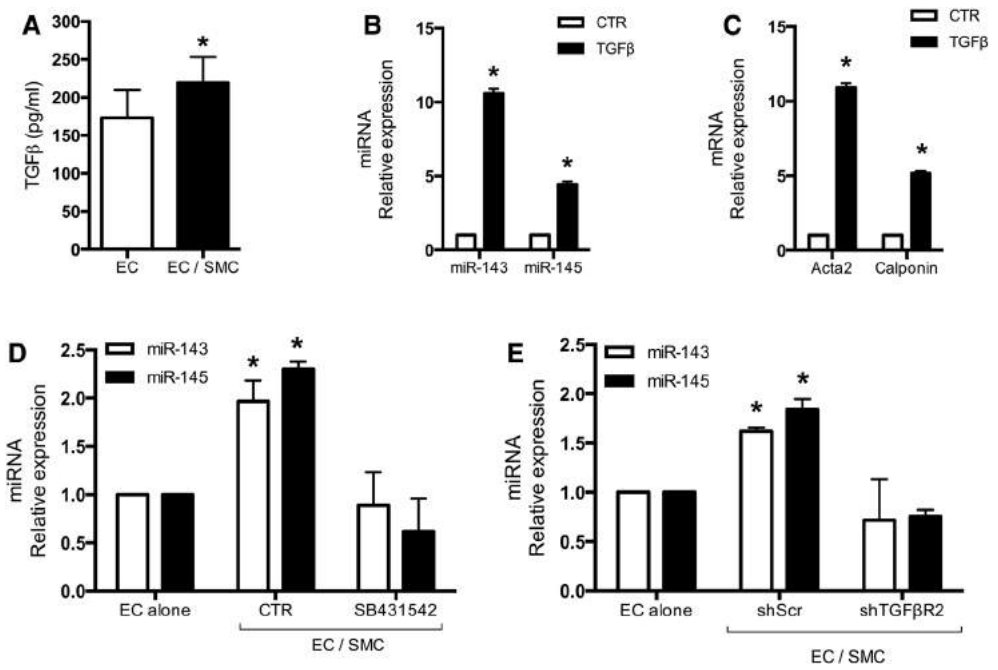

Figure 2. Transforming growth factor (TGF) β triggers the transfer of miR-143 and miR-145 from smooth muscle cells (SMCs) to endothelial cells (ECs). A, Medium from EC/SMC (human umbilical vein endothelial cells [HUVEC]/murine SMCs) coculture was collected after 24 hours and the level of hTGFβ1 measured by ELISA. **B**, Mature miR-143 and miR-145 and (**C**) smooth muscle differentiation genes (*Acta2* and *Calponin*) were analyzed in SMCs treated with 10 ng/mL of TGFβ for 24 hours. **D**, MiR-143 and miR-145 were measured in ECs (H5V) after coculture with SMCs without or with the TGFβ inhibitor SB431542, at 24 hours, (**E**) and in ECs (HUVEC) with SMCs transduced with a lentivirus expressing an shRNA scrambled sequence (shScr) or shRNA against TGFβ receptor 2 (shTGFβR2). Measurements in **A** and error bars calculated as propagated SEM of triplicate measurements from each experiment. Data for **B**–**E** were plotted and analyzed as described in Figure 1. **P*<0.05 (each experiment was replicated at least 3×). CTR indicates control.

membranes. The purity of ECs (which reached 99%) was determined by staining the separated cells for α smooth muscle actin and performing fluorescence-activated cell sorter analysis (data not shown), as previously reported by other groups.[38] We found that inhibiting coculture cell contact with LatA (Online Figure IVA) reduced the transfer of miR-143/145 from SMCs to ECs (Figure 3C).

TNTs are heterogeneous structures that express F-actin and other proteins.[39] When we analyzed the origin of the TNTs with cell type–specific staining, we found that they grew out of ECs and SMCs, and formed homocellular and heterocellular contacts (Figure 3D). We detected the presence of tubulin, F-actin, and the small GTPase Cdc42 in TNTs, but never the expression of Cx43 (Online Figure IVB).

We then studied TNT formation using scanning ion conductance microscopy. After seeding, the cells created TNT contacts in <30 minutes (Figure 3F, top). Detailed analysis of the TNT formation profile indicated that the total cell volume was not changed and that there was a continuous membrane profile at the cell-to-cell junction point, indicative of direct cytoplasmic communication between the interacting cells (Figure 3F, bottom). This was further supported at the ultrastructural level by scanning electron microscopy (Online Figure V).

Finally, to confirm that TNTs vehicle miR-143/145 from SMCs to ECs, we transduced primary SMCs with fluorescently labeled miRNA mimics and then cocultured them with ECs: fluorescent signals were indeed detected in TNTs and ECs (Figure 3E and Online Movies I and II). Together, these results strongly support the notion that, after the activation of SMCs by ECs, miR-143 and miR-145 are transferred from SMCs to ECs via TNTs.

Antiangiogenic Effects of miR-143/145 on ECs

Angiogenesis is a complex process in which a tight coordination of cues (cytokines, growth factors, etc.) controls EC migration and proliferation.[40,41] When EC-lined tubes are formed, the structures are stabilized by supporting cells, such as SMCs and pericytes.[42] In this state, ECs do not possess strong angiogenic capabilities, so cell growth potential is limited.[43]

Because we observed that the TGFβ pathway, which is important for vessel stabilization,[6,25] significantly regulated miR-143/145 transfer to ECs, we asked whether miR-143/145 might have an antiangiogenic role on ECs. To test this hypothesis, we performed a vessel formation assay by plating ECs overexpressing either miR-143 or miR-145 on matrigel and then measuring their ability to form vessel-like structures. The levels of overexpressed miRNA were similar to those observed after direct coculture and separation with anti-Pecam1 beads (Online Figure VIA). As expected, miR-143– and miR-145–expressing ECs lost their angiogenic potential compared with nonexpressing controls (Figure 4A). To demonstrate the functional capacity of the transferred miR-143/145 in cocultured ECs, we repeated the experiments by coculturing ECs with either WT SMCs or miR-143/145-KO SMCs on matrigel. Although there was no difference in vessel formation after 6 hours of coculture (data not shown), ECs cocultured with WT SMCs lost their ability to form vessels after

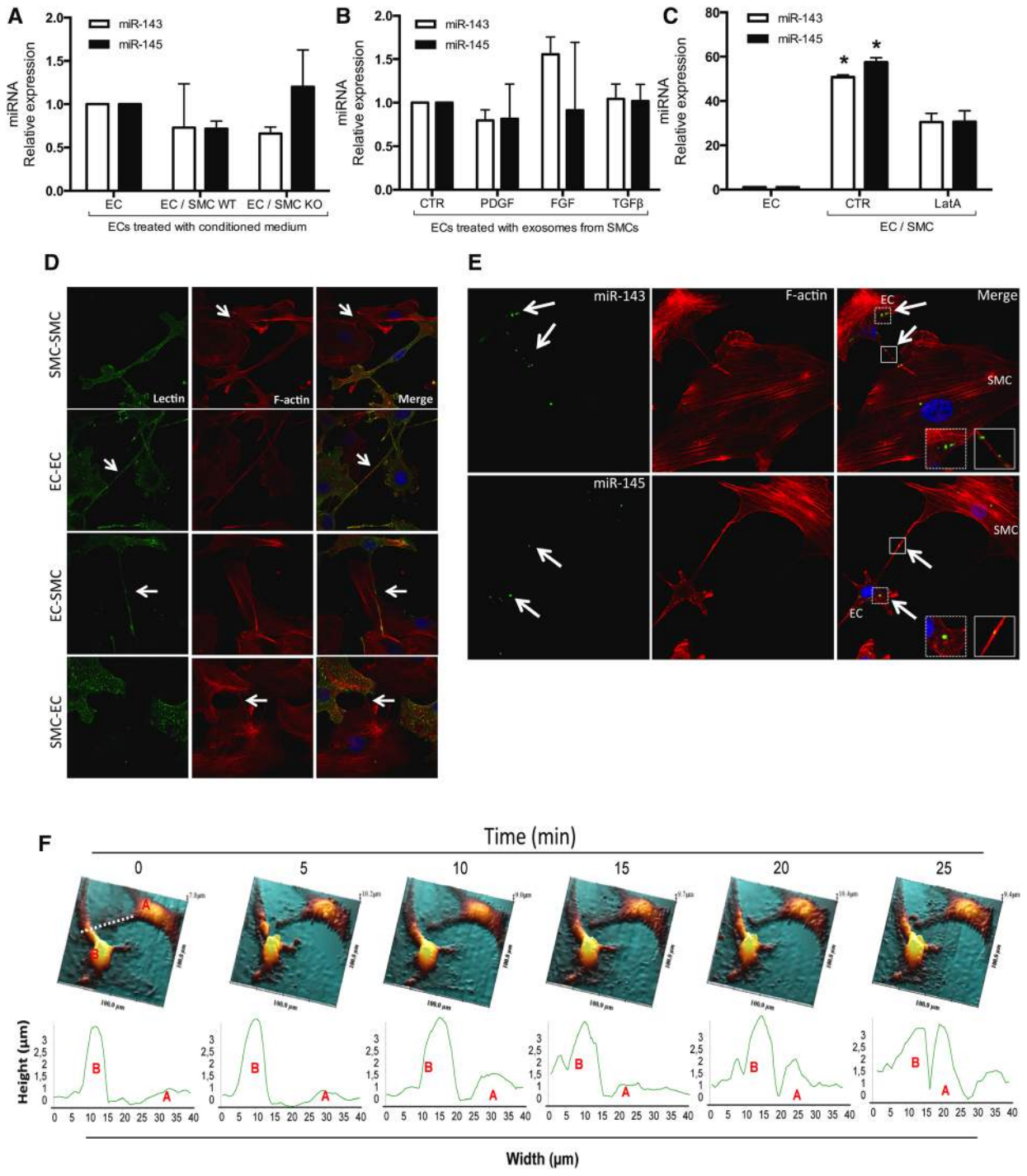

Figure 3. Mechanism of miR-143 and miR-145 transfer from smooth muscle cells (SMCs) and endothelial cells (ECs). Levels of miR-143 and miR-145 were analyzed: (**A**) in ECs (human umbilical vein endothelial cells [HUVEC]) incubated 24 hours with conditioned medium from cocultures of ECs and wild-type (WT) or miR-143/145 knockout (KO) SMCs; (**B**) in ECs (HUVEC) challenged with exosomes purified from SMCs treated with platelet-derived growth factor (PDGF), fibroblast growth factor, or transforming growth factor (TGF) β; and (**C**) in ECs (HUVECs) first cocultured with WT SMCs, with or without Latrunculin A (LatA) for 24 hours, and then purified using anti-Pecam1 magnetic beads. **D**, Confocal images of Lectin- and F-actin–stained ECs and WT SMCs for identification of tunneling nanotubes (TNT); (**E**) Alexa-488-miR-143 and Alexa-488-miR-145 in TNTs between SMCs and ECs: white arrows indicate fluorescent miRNA mimics within TNTs and ECs. **F**, Time-course of TNT formation (range, 40 μm). **Top**, Scanning ion conductance microscopy color-coded topographical images taken in loop mode every 5 minutes. **Bottom**, height profiles along the dashed green line, showing a nanotube forming from an SMC (**A**) and fusing with an EC (**B**). Data for **A**–**C** were plotted and analyzed as described in Figure 1. *P<0.05 (each experiment was replicated at least 3×). CTR indicates control.

16 hours (Figure 4B), confirming the antiangiogenic role of miR-143/145. In contrast, coculture with miR-143/145-KO SMCs did not inhibit the formation of capillary-like structures by ECs. Coherently, ECs transduced with anti–miR-143 and anti–miR-145 locked nucleic acid oligonucleotides and then cocultured with WT SMCs had an increased capacity to form

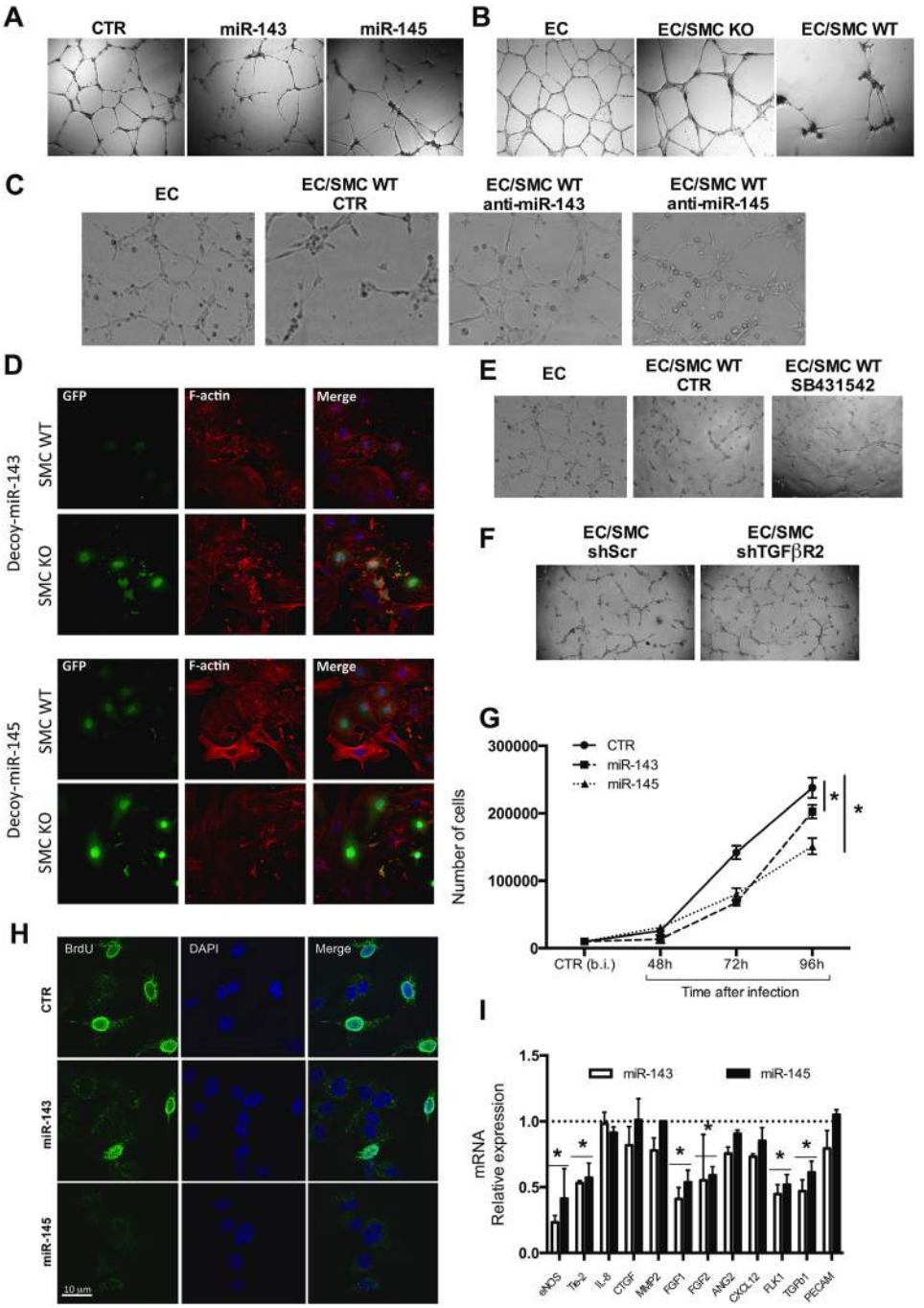

Figure 4. Effects of miR-143 and miR-145 on endothelial cells (ECs). 96- or 48-well plates were precoated with GelTrex and EC tube formation assay performed with: (**A**) control (CTR) ECs (human umbilical vein endothelial cells [HUVEC]) or ECs overexpressing miR-143 or miR-145; (**B**) ECs (HUVECs) alone or in coculture with wild-type (WT) or miR-143/145 knockout (KO) smooth muscle cells (SMCs); and (**C**) ECs (HUVECs) transduced with anti–miR-143 and anti–miR-145 locked nucleic acid oligonucleotides and then cocultured with WT or miR-143/145-KO SMCs (as control). **D**, ECs transduced with a decoy system: Decoy-miR-143 or decoy-miR-145 ECs (H5V) were cocultured with WT or miR-143/145 KO SMCs and stained for F-actin after 72 hours. Tube formation assay on ECs (HUVECs) isolated from coculture (**E**) with WT SMCs without or with the transforming growth factor (TGF) β inhibitor SB431542 or (**F**) with WT SMCs transduced with a lentivurs expressing an shRNA sequence scrambled or against TGFβR2. **G**, Growth curve of CTR ECs and those overexpressing miR-143 or miR-145 at different time points. **H**, BrdU incorporation in CTR ECs and ECs overexpressing miR-143 or miR-145, and relative quantification (magnification: ×20). **I**, quantitative reverse transcription polymerase chain reaction analysis of endothelial markers in CTR ECs and ECs overexpressing miR-143 or miR-145. The threshold (obtained from CTR ECs) is indicated by the dotted line. Error bars in **C** and **D** were calculated as propagated SEM of triplicate measurements from each experiment. Data in **E** were plotted and analyzed as described in Figure 1. **P*<0.05 (each experiment was replicated at least 3×). b.i. indicates before infection.

vessel-like structures on matrigel (Figure 4C). To further corroborate these findings, we generated 2 decoy systems in which synthetic untranslated regions harboring 2 tandem miR-143 or miR-145 complementary sequences were placed 3′ to the GFP gene. ECs transduced with these decoys were cocultured with either WT or miR-143/145 KO SMCs: after

72 hours, a clear reduction of the GFP signal was observed in EC/WT SMC cocultures compared with the EC/KO SMC ones (Figure 4D; Online Figure VIB). Moreover, ECs cultured with WT SMCs treated with the TGFβ inhibitor SB431542 or SMCs transduced with an shRNA sequence against TGFβR2 had an increased ability to form capillary-like structures on matrigel (Figure 4E and 4F).

In addition, ECs overexpressing miR-143 or miR-145 had a reduced proliferation index, as assessed by growth curve and BrdU incorporation analyses (Figure 4G and 4H; Online Figure VIC). To further validate the antiangiogenic role of these 2 miRNAs in ECs, we measured the mRNA levels of different EC angiogenic markers. We found a significant downregulation of many of them (Figure 4I). Taken together, this set of experiments indicates that the miR-143/145 cluster regulates EC growth properties upon direct contact with SMCs during vessel formation.

Identification of miR-143 and miR-145 Targets in ECs

Having established that the transfer of miR-143 and miR-145 from SMCs exerts a powerful biological effect on ECs by inhibiting their growth, we sought to identify the targets of these miRNAs in ECs. Through a bioinformatics approach, we found that hexokinase II (*HKII*) and integrin β 8 (*ITGβ8*) were potential binding partners for miR-143 and miR-145, respectively. These genes have highly conserved seed sequences (Online Figure VID). Transduction of primary ECs with lentiviral miR-143– and miR-145–encoding vectors decreased the abundance of the target proteins and their mRNA levels (Figure 5A and 5B). Luciferase assay with 3′ untranslated region–binding sites confirmed that *HKII* and *ITGβ8* mRNAs were directly targeted by miR-143 and miR-145; deregulation was not observed when the seed sequences were mutated (Figure 5C). In addition, binding affinity of the 2 miRNAs to their targets was confirmed by Ago2-immunoprecipitation experiments (Figure 5D).

We then tested whether HKII and ITGβ8 were implicated in angiogenic regulation in ECs. In loss-of-function experiments, we determined that primary ECs knocked-down for *HKII* and *ITGβ8* had a reduced capacity to form vessel-like structures when cultured on matrigel (Figure 5E), and a reduced proliferation capacity (Figure 5F and 5G; Online Figure VIE). Thus, *HKII* and *ITGβ8* are 2 important miR-143/145 targets that regulate the angiogenic capability of ECs.

Transfer of miR-143/145 From SMCs to ECs Ex Vivo and In Vivo

To determine whether the in vitro results were applicable also in an ex vivo setting, we performed experiments using aortas excised from WT mice. Vessels were cultured in normal medium for 24 hours and then, after 16 hours of serum starvation, were treated with or without TGFβ for 24 hours. Aortas were then dissected and digested for EC isolation with anti-Pecam1 magnetic beads. The purity of EC separation was >99% (Online Figure VIIA and VIIB), and a comparison of *Pecam1* and different smooth muscle differentiation marker (*Acta2*, *Calponin*, and *Myh6*) mRNA levels in the positive and negative fractions confirmed the quality of the separation process (Online Figure VIIIA and VIIIB). MiR-143 and miR-145 were found significantly increased in isolated ECs from TGFβ-treated vessels, confirming the in vitro results (Figure 6A). No differences in pri-miR-143/145 levels were detected (Figure 6B), suggesting that TGFβ triggers only the transfer of mature miR-143/145 from SMCs to ECs.

To further corroborate these findings in vivo, we used our mouse model, in which the miR-143/145 cluster can be specifically deleted in the SMC layer on induction with tamoxifen (Online Figure VIIIC and VIIID). Trans-aortic constriction-induced pressure overload increased miR-143/145 expression in the endothelium of coronary arteries of WT mice, an effect absent in the SMC-specific miR-143/145 KO mice (Figure 6C). *HKII* and *ITGβ8*, the 2 identified miR-143/145 targets, were increased in the EC layer of KO vessels when compared with WT (Figure 6D and 6E). We also found that in vivo migration was significantly increased in ECs from KO mice when we performed a matrigel plug assay (Figure 6F; Online Figure VIIIE).

As a whole, these ex vivo and in vivo results further support the notion that the TGFβ signaling cascade triggers the transfer of the miR-143/145 cluster to ECs from SMCs, and that this transfer reduces EC migration.

Discussion

Vasculogenesis is the process by which mesoderm-derived endothelial precursor cells (angioblasts) form de novo vessels; it is responsible for the formation of the first, primitive blood vessels in the embryo. In contrast, physiological and pathological blood vessel growth later on in life is predominantly, if not exclusively, achieved through angiogenesis-dependent mainly on mature ECs.[44] In adulthood, the formation and function of these vessels support the life of organs; the functional and structural organization of vessels are maintained by the direct interaction between ECs and mural cells. However, ECs are highly heterogeneous in terms of functional properties and gene expression profiles. This heterogeneity depends on the differentiation and proliferation status.[45]

The miR-143/145 cluster has been observed to play a fundamental role governing SMC differentiation during physiological and pathological events.[8,10,15–18] Beside its ability to regulate SMC homeostasis, it is still not well understood how the miR-143/145 cluster regulates EC functions. In this report, we demonstrate that the modulation of the angiogenic potential of ECs is also due to the direct transfer of miR-143/145 from SMCs. It is known that EC/SMC contact triggers SMC activation through the TGFβ pathway,[25] but the effect of stimulated SMCs on ECs is still unclear. Here, we confirm that the level of miR-143/145 is increased in differentiated SMCs,[26] and that this triggers the transfer of these small RNAs to neighboring ECs. Furthermore, overexpression of either miR-143 or miR-145 in ECs reduced the ability of ECs to form capillary-like structures and decreased their proliferation index. This effect was further confirmed in other experiments, such as coculture of ECs with WT SMCs or miR-143/145 KO SMCs: as a matter of fact, WT, but not KO, SMCs were able to reduce the angiogenic capacity of ECs.

This phenomenon might have implications also for tumor biology. Many studies have shown the role of the miR-143/145 cluster in cancer development.[46–48] Under pathological

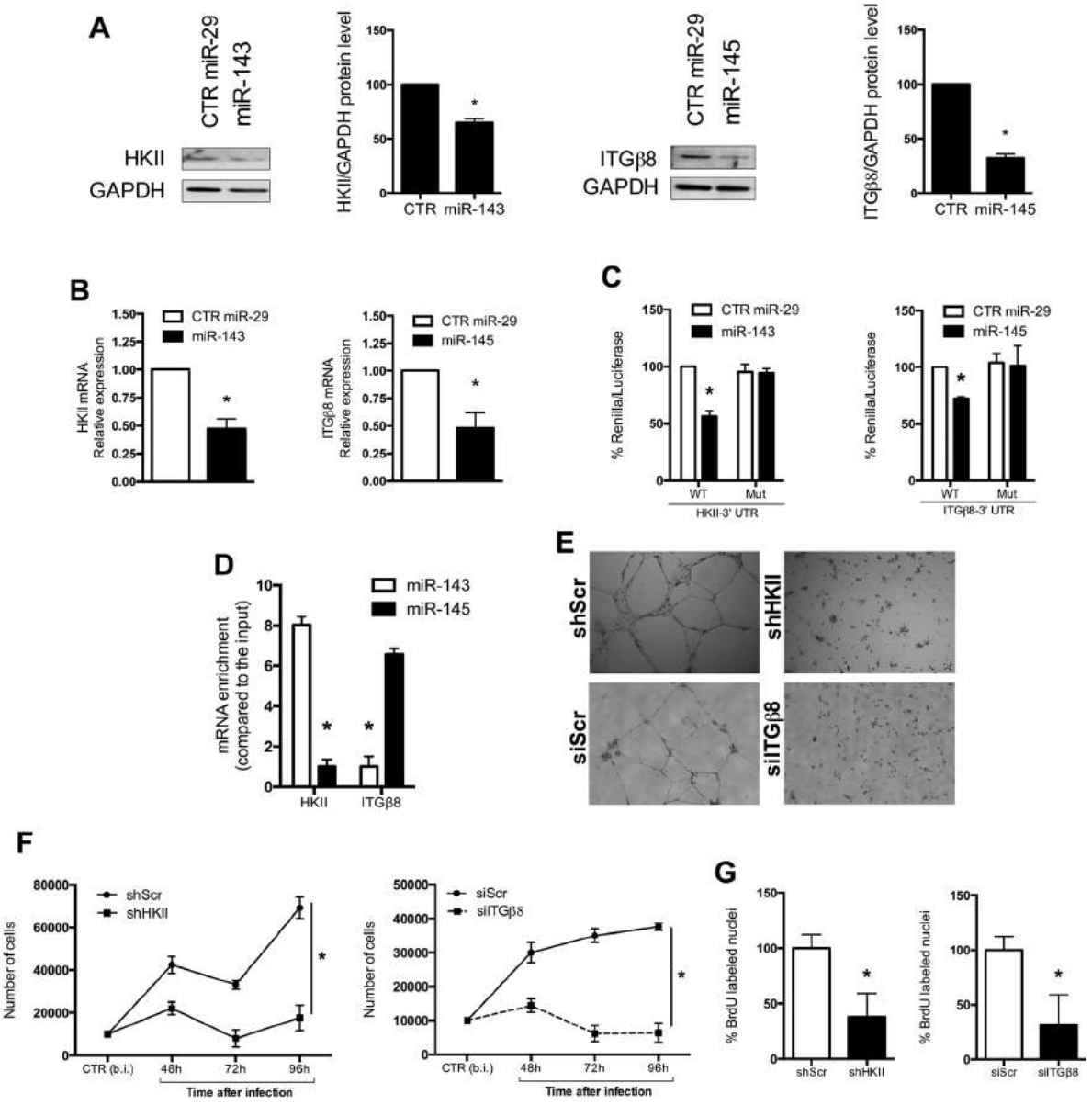

Figure 5. Targets of miR-143 and miR-145 in endothelial cells (ECs). A, Representative immunoblots for the target genes hexokinase II (HKII) and integrin β 8 (ITGβ8) in control (CTR) ECs (H5V) and ECs overexpressing miR-143, miR-145, or miR-29, and relative quantification normalized to GAPDH. **B**, RNA analysis of *HKII* and *ITGβ8* RNAs with quantitative reverse transcription polymerase chain reaction (qRT-PCR). **C**, Luciferase reporter assay (all measurements were calculated as percent of control (wild-type [WT] 3′ untranslated region [UTR]) and error bars calculated as propagated SEM of triplicate measurements from each experiment) on ECs (H5V), performed by cotransfection of (20 nmol/L) miR-143, miR-145, or CTR (miR-29) with a renilla reporter gene linked to (10 ng) wild-type (WT) or mutated (Mut) 3′ UTRs of HKII and ITGβ8. **D**, miR-143 or miR-145 mimics were transfected in ECs (H5V) and 48 hours later cells were lysed for Ago2-immunoprecipitation assay. RNA levels for *HKII* and *ITGβ8* were analyzed by qRT-PCR. ECs (HUVEC [human umbilical vein endothelial cells]) were transduced with shSCR, shHKII, siSCR, or siITGβ8 and assayed for: (**E**) tube formation; (**F**) growth curve; and (**G**) BrdU incorporation. Data in **B** and **D** were plotted and analyzed, respectively as described in Figure 1. **P*<0.05 (each experiment was replicated at least 3×).

conditions, such as wound healing and malignancies, angiogenesis is in fact reactivated.[49] As tumor cells grow, the formation of new immature blood vessels increases together with the request for supplies. In the normal vasculature, pericytes and SMCs are important for the stabilization of ECs and mediate EC survival together with the maturation of the vessels; mural cells modulate these events by direct cell contact and paracrine signaling.[50] In contrast, pericytes and SMCs are usually absent in the tumor vasculature or have loose associations with ECs, leaving most of the tumor's microvessels immature.[42,51,52] On the basis of our data, it can be speculated that to maintain the proangiogenic phenotype of ECs, the level of miR-143/145 in the surrounding SMCs has to be low. Interestingly, tumors frequently have decreased levels of these miRNAs compared with normal samples of the same tissue.[46,48] Thus, it is possible that downregulation of the miR-143/145 cluster is associated with increased angiogenesis in tumors because the stabilizing effect on ECs is decreased or lost.

Another interesting aspect of our results relates to the role of the TNT plasma-membrane structures in mediating the

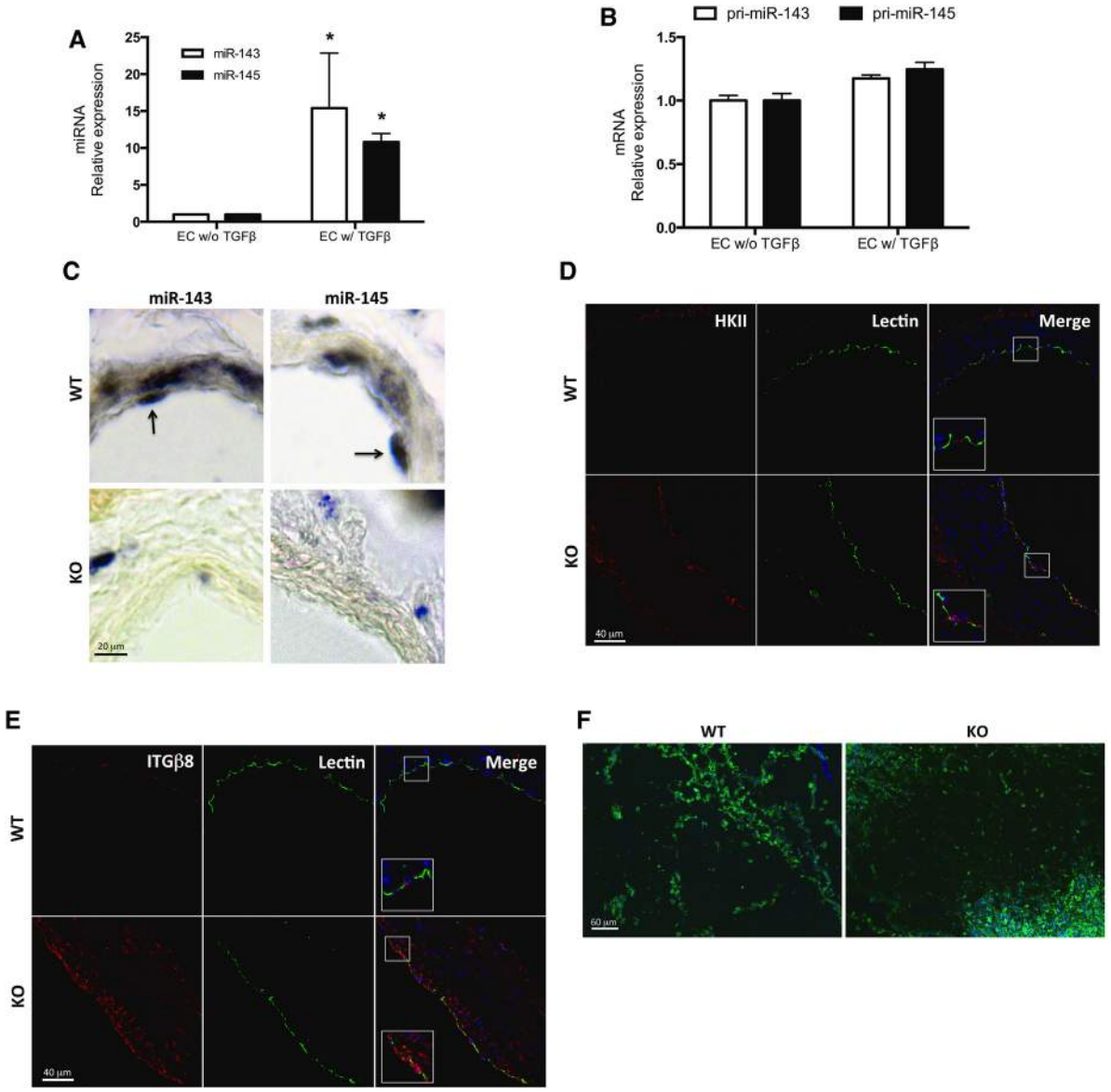

Figure 6. miR-143/145 transfer ex vivo and in vivo. Quantitative polymerase chain reaction for (**A**) mature miR-143 and miR-145, and (**B**) pri-miR-143 and pri-miR-145 in the endothelial cell (EC) fraction of wild-type (WT) vessels exposed to transforming growth factor (TGF) β. **C**, In situ hybridization for miR-143 and miR-145 in coronary arteries of WT (cre+) and miR-143/145 knockout (KO; floxed/cre+) mice after transaortic constriction; black arrows indicate positive ECs (magnification: ×100). **D** and **E**, Staining for hexokinase II (HKII) and integrin β 8 (ITGβ8) in WT and KO aortas after tamoxifen injection (magnification: ×20). **F**, Representative images of Lectin (green) and 4′,6-diamidino-2-phenylindole (blue) staining of matrigel plugs implanted into mice of the indicated genotypes (magnification: ×4). Data in **A** and **B** were plotted and analyzed as described in Figure 1. **P*<0.05 (each experiment was replicated at least 3×).

transfer of miRNAs in cell-to-cell communication. TNTs are line-like membrane tubes able to connect 2 cells. The diameter of TNTs ranges from 50 to 200 nm and some are as long as the diameter of some cells. These structures have been observed in many different cell types, such as tumor cells, natural killer (NK) cells, cardiomyocytes, and ECs.[35,36,53] That TNTs might mediate the transfer of the miR-143/145 cluster from SMCs to ECs is here demonstrated by various lines of evidence (1) exosomes or other secreted structures are not implicated in the transfer; (2) inhibition of cell contact through gap junction inhibition does not reduce miR-143/145 passage to ECs; (3) with the use of a TNT inhibitor (LatA), we were able to significantly reduce miRNA transfer from SMCs to ECs, demonstrating that these structures are probably important routes for the passage of small RNAs between cells; and (4) observation of fluorescent miR-143 and miR-145 in TNTs.

We also demonstrate that inhibition of 2 direct EC targets of miR-143/145, *HKII* and *ITGβ8*, is sufficient for reducing the angiogenic phenotype of ECs. These 2 targets were previously demonstrated to be regulated by the miR-143/145 cluster in cancer cells[54] and human corneal epithelial cells,[55] respectively. Our data, although confirming the role of miR-143/145 in regulating these 2 targets also in ECs, demonstrate their importance in modulating EC biology.

In vessel maturation and stabilization, the specialization of vessel-wall cells is an important, yet not totally

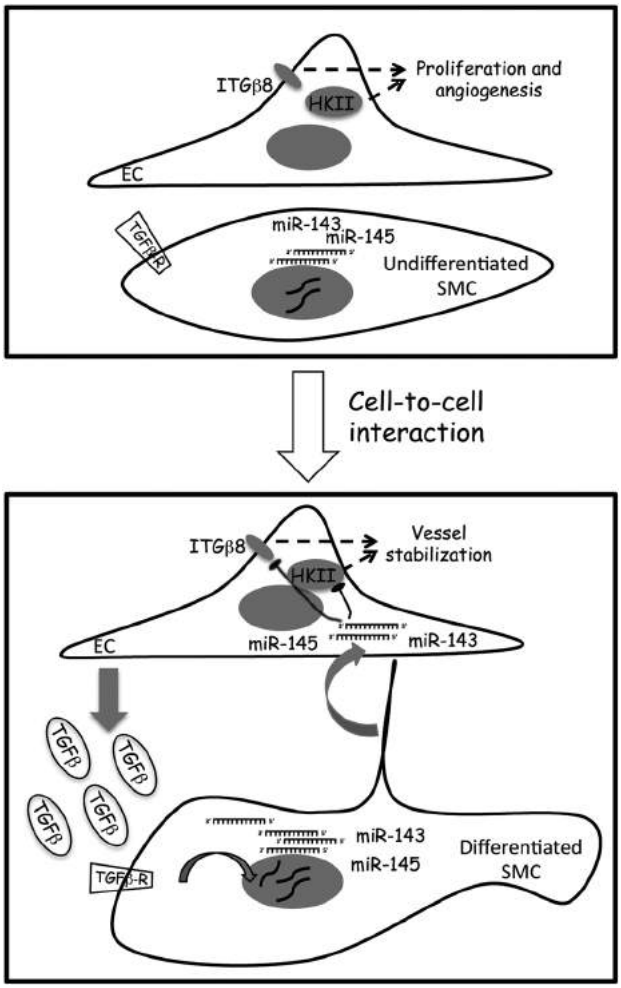

Figure 7. Model of the role of miR-143 and miR-145 in endothelial cells (ECs) on direct transfer from smooth muscle cells (SMCs). After contact with SMCs, ECs secrete transforming growth factor (TGF) β. This, in turn, stimulates SMC differentiation and miR-143/145 upregulation, triggering also the transfer of the miRNAs to ECs via tunneling nanotubes. In ECs, miR-143 and miR-145 negatively modulate hexokinase II (HKII) and integrin β 8 (ITGβ8) expression, leading to reduced angiogenic capabilities and a stabilization of the endothelium.

understood, event.[56] Vessel maturation involves the phenotypic specialization of ECs and mural cells, stabilized by the production of extracellular matrix. This process is guided mainly by homotypic and heterotypic cell contacts.[56] Different pathways are involved in this biological process: sphingosine-1-phosphate-1 endothelial differentiation sphingolipid G-protein–coupled receptor-1,[57] Ang1-Tie2,[58] platelet-derived growth factor B–-PDGF receptor-β,[59] and TGFβ.[60] Apart from these indications, there is scant information on the involvement of miRNAs in EC/SMC communication during vessel stabilization. Here, we prove also in vivo that miR-143/145 cluster modulates EC function through direct transfer from SMCs.

Our work demonstrates the effect of the miR-143/145 cluster on EC stabilization, a process that depends on the direct transfer of these miRNAs from differentiated SMCs induced by TGFβ (Figure 7). This finding could have relevant implications for pathological and therapeutic angiogenesis.

Acknowledgments

We thank Diego Morone and Andrea Doni for support with microscopy experiments; Paolo Somma and Achille Anselmo for fluorescence-activated cell sorter analysis; Paola Lagonegro and Tiziano Rimoldi for scanning electron microscopy; Michael V.G Latronico for critically reviewing the article; and Pierluigi Carullo and Alessandra Rodanò for animal studies.

Sources of Funding

This work was supported by grants from the Italian Ministry of Health (No. GR2010_2302354) and Marie Curie Action (No. PIRG08-GA-2010–276993) to L. Elia; and an Advanced Grant (CardioEpigen, No. 294609) from the European Research Council to G. Condorelli.

Disclosures

None.

References

1. Bonetti PO, Lerman LO, Lerman A. Endothelial dysfunction: a marker of atherosclerotic risk. *Arterioscler Thromb Vasc Biol*. 2003;23:168–175.
2. Ross R. Atherosclerosis–an inflammatory disease. *N Engl J Med*. 1999;340:115–126. doi: 10.1056/NEJM199901143400207.
3. Velazquez OC. Angiogenesis and vasculogenesis: inducing the growth of new blood vessels and wound healing by stimulation of bone marrow-derived progenitor cell mobilization and homing. *J Vasc Surg*. 2007;45(suppl A):A39–A47. doi: 10.1016/j.jvs.2007.02.068.
4. Benjamin LE, Hemo I, Keshet E. A plasticity window for blood vessel remodelling is defined by pericyte coverage of the preformed endothelial network and is regulated by PDGF-B and VEGF. *Development*. 1998;125:1591–1598.
5. Abramsson A, Lindblom P, Betsholtz C. Endothelial and nonendothelial sources of PDGF-B regulate pericyte recruitment and influence vascular pattern formation in tumors. *J Clin Invest*. 2003;112:1142–1151. doi: 10.1172/JCI18549.
6. Jain RK. Molecular regulation of vessel maturation. *Nat Med*. 2003;9:685–693. doi: 10.1038/nm0603-685.
7. Bartel DP. MicroRNAs: genomics, biogenesis, mechanism, and function. *Cell*. 2004;116:281–297.
8. Elia L, Quintavalle M, Zhang J, Contu R, Cossu L, Latronico MV, Peterson KL, Indolfi C, Catalucci D, Chen J, Courtneidge SA, Condorelli G. The knockout of miR-143 and -145 alters smooth muscle cell maintenance and vascular homeostasis in mice: correlates with human disease. *Cell Death Differ*. 2009;16:1590–1598. doi: 10.1038/cdd.2009.153.
9. Quintavalle M, Condorelli G, Elia L. Arterial remodeling and atherosclerosis: miRNAs involvement. *Vascul Pharmacol*. 2011;55:106–110. doi: 10.1016/j.vph.2011.08.216.
10. Quintavalle M, Elia L, Condorelli G, Courtneidge SA. MicroRNA control of podosome formation in vascular smooth muscle cells in vivo and in vitro. *J Cell Biol*. 2010;189:13–22. doi: 10.1083/jcb.200912096.
11. Condorelli G, Latronico MV, Cavarretta E. microRNAs in cardiovascular diseases: current knowledge and the road ahead. *J Am Coll Cardiol*. 2014;63:2177–2187. doi: 10.1016/j.jacc.2014.01.050.
12. Vickers KC, Palmisano BT, Shoucri BM, Shamburek RD, Remaley AT. MicroRNAs are transported in plasma and delivered to recipient cells by high-density lipoproteins. *Nat Cell Biol*. 2011;13:423–433. doi: 10.1038/ncb2210.
13. Zernecke A, Bidzhekov K, Noels H, Shagdarsuren E, Gan L, Denecke B, Hristov M, Köppel T, Jahantigh MN, Lutgens E, Wang S, Olson EN, Schober A, Weber C. Delivery of microRNA-126 by apoptotic bodies induces CXCL12-dependent vascular protection. *Sci Signal*. 2009;2:ra81. doi: 10.1126/scisignal.2000610.
14. Hergenreider E, Heydt S, Tréguer K, Boettger T, Horrevoets AJ, Zeiher AM, Scheffer MP, Frangakis AS, Yin X, Mayr M, Braun T, Urbich C, Boon RA, Dimmeler S. Atheroprotective communication between endothelial cells and smooth muscle cells through miRNAs. *Nat Cell Biol*. 2012;14:249–256. doi: 10.1038/ncb2441.
15. Boettger T, Beetz N, Kostin S, Schneider J, Krüger M, Hein L, Braun T. Acquisition of the contractile phenotype by murine arterial smooth muscle cells depends on the Mir143/145 gene cluster. *J Clin Invest*. 2009;119:2634–2647. doi: 10.1172/JCI38864.

16. Cordes KR, Sheehy NT, White MP, Berry EC, Morton SU, Muth AN, Lee TH, Miano JM, Ivey KN, Srivastava D. miR-145 and miR-143 regulate smooth muscle cell fate and plasticity. *Nature*. 2009;460:705–710. doi: 10.1038/nature08195.
17. Xin M, Small EM, Sutherland LB, Qi X, McAnally J, Plato CF, Richardson JA, Bassel-Duby R, Olson EN. MicroRNAs miR-143 and miR-145 modulate cytoskeletal dynamics and responsiveness of smooth muscle cells to injury. *Genes Dev*. 2009;23:2166–2178. doi: 10.1101/gad.1842409.
18. Norata GD, Pinna C, Zappella F, Elia L, Sala A, Condorelli G, Catapano AL. MicroRNA 143-145 deficiency impairs vascular function. *Int J Immunopathol Pharmacol*. 2012;25:467–474.
19. Kohlstedt K, Trouvain C, Boettger T, Shi L, Fisslthaler B, Fleming I. AMP-activated protein kinase regulates endothelial cell angiotensin-converting enzyme expression via p53 and the post-transcriptional regulation of microRNA-143/145. *Circ Res*. 2013;112:1150–1158. doi: 10.1161/CIRCRESAHA.113.301282.
20. Shevchuk AI, Novak P, Takahashi Y, Clarke R, Miragoli M, Babakinejad B, Gorelik J, Korchev YE, Klenerman D. Realizing the biological and biomedical potential of nanoscale imaging using a pipette probe. *Nanomedicine (Lond)*. 2011;6:565–575. doi: 10.2217/nnm.10.154.
21. Miragoli M, Yacoub MH, El-Hamamsy I, Sanchez-Alonso JL, Moshkov A, Mongkoldhumrongkul N, Padala M, Paramagurunathan S, Sarathchandra P, Korchev YE, Gorelik J, Chester AH. Side-specific mechanical properties of valve endothelial cells. *Am J Physiol Heart Circ Physiol*. 2014;307:H15–H24. doi: 10.1152/ajpheart.00228.2013.
22. Elia L, Contu R, Quintavalle M, Varrone F, Chimenti C, Russo MA, Cimino V, De Marinis L, Frustaci A, Catalucci D, Condorelli G. Reciprocal regulation of microRNA-1 and insulin-like growth factor-1 signal transduction cascade in cardiac and skeletal muscle in physiological and pathological conditions. *Circulation*. 2009;120:2377–2385. doi: 10.1161/CIRCULATIONAHA.109.879429.
23. Isakson BE, Duling BR. Heterocellular contact at the myoendothelial junction influences gap junction organization. *Circ Res*. 2005;97:44–51. doi: 10.1161/01.RES.0000173461.36221.2e.
24. Chang SF, Chen LJ, Lee PL, Lee DY, Chien S, Chiu JJ. Different modes of endothelial-smooth muscle cell interaction elicit differential β-catenin phosphorylations and endothelial functions. *Proc Natl Acad Sci U S A*. 2014;111:1855–1860. doi: 10.1073/pnas.1323761111.
25. Walshe TE, Saint-Geniez M, Maharaj AS, Sekiyama E, Maldonado AE, D'Amore PA. TGF-beta is required for vascular barrier function, endothelial survival and homeostasis of the adult microvasculature. *PLoS One*. 2009;4:e5149. doi: 10.1371/journal.pone.0005149.
26. Long X, Miano JM. Transforming growth factor-beta1 (TGF-beta1) utilizes distinct pathways for the transcriptional activation of microRNA 143/145 in human coronary artery smooth muscle cells. *J Biol Chem*. 2011;286:30119–30129. doi: 10.1074/jbc.M111.258814.
27. Inman GJ, Nicolás FJ, Callahan JF, Harling JD, Gaster LM, Reith AD, Laping NJ, Hill CS. SB-431542 is a potent and specific inhibitor of transforming growth factor-beta superfamily type I activin receptor-like kinase (ALK) receptors ALK4, ALK5, and ALK7. *Mol Pharmacol*. 2002;62:65–74.
28. Micalizzi DS, Christensen KL, Jedlicka P, Coletta RD, Barón AE, Harrell JC, Horwitz KB, Billheimer D, Heichman KA, Welm AL, Schiemann WP, Ford HL. The Six1 homeoprotein induces human mammary carcinoma cells to undergo epithelial-mesenchymal transition and metastasis in mice through increasing TGF-beta signaling. *J Clin Invest*. 2009;119:2678–2690. doi: 10.1172/JCI37815.
29. Lin T, Ambasudhan R, Yuan X, Li W, Hilcove S, Abujarour R, Lin X, Hahm HS, Hao E, Hayek A, Ding S. A chemical platform for improved induction of human iPSCs. *Nat Methods*. 2009;6:805–808. doi: 10.1038/nmeth.1393.
30. Ikushima H, Todo T, Ino Y, Takahashi M, Miyazawa K, Miyazono K. Autocrine TGF-beta signaling maintains tumorigenicity of glioma-initiating cells through Sry-related HMG-box factors. *Cell Stem Cell*. 2009;5:504–514. doi: 10.1016/j.stem.2009.08.018.
31. Lund LR, Riccio A, Andreasen PA, Nielsen LS, Kristensen P, Laiho M, Saksela O, Blasi F, Danø K. Transforming growth factor-beta is a strong and fast acting positive regulator of the level of type-1 plasminogen activator inhibitor mRNA in WI-38 human lung fibroblasts. *EMBO J*. 1987;6:1281–1286.
32. Nakao A, Afrakhte M, Morén A, Nakayama T, Christian JL, Heuchel R, Itoh S, Kawabata M, Heldin NE, Heldin CH, ten Dijke P. Identification of Smad7, a TGFbeta-inducible antagonist of TGF-beta signalling. *Nature*. 1997;389:631–635. doi: 10.1038/39369.
33. Lim PK, Bliss SA, Patel SA, Taborga M, Dave MA, Gregory LA, Greco SJ, Bryan M, Patel PS, Rameshwar P. Gap junction-mediated import of microRNA from bone marrow stromal cells can elicit cell cycle quiescence in breast cancer cells. *Cancer Res*. 2011;71:1550–1560. doi: 10.1158/0008-5472.CAN-10-2372.
34. Aucher A, Rudnicka D, Davis DM. MicroRNAs transfer from human macrophages to hepato-carcinoma cells and inhibit proliferation. *J Immunol*. 2013;191:6250–6260. doi: 10.4049/jimmunol.1301728.
35. Watkins SC, Salter RD. Functional connectivity between immune cells mediated by tunneling nanotubules. *Immunity*. 2005;23:309–318. doi: 10.1016/j.immuni.2005.08.009.
36. Koyanagi M, Brandes RP, Haendeler J, Zeiher AM, Dimmeler S. Cell-to-cell connection of endothelial progenitor cells with cardiac myocytes by nanotubes: a novel mechanism for cell fate changes? *Circ Res*. 2005;96:1039–1041. doi: 10.1161/01.RES.0000168650.23479.0c.
37. Thayanithy V, Dickson EL, Steer C, Subramanian S, Lou E. Tumor-stromal cross talk: direct cell-to-cell transfer of oncogenic microRNAs via tunneling nanotubes. *Transl Res*. 2014;164:359–365. doi: 10.1016/j.trsl.2014.05.011.
38. Lilly B, Kennard S. Differential gene expression in a coculture model of angiogenesis reveals modulation of select pathways and a role for Notch signaling. *Physiol Genomics*. 2009;36:69–78. doi: 10.1152/physiolgenomics.90318.2008.
39. Abounit S, Zurzolo C. Wiring through tunneling nanotubes–from electrical signals to organelle transfer. *J Cell Sci*. 2012;125:1089–1098. doi: 10.1242/jcs.083279.
40. Davis GE, Bayless KJ, Mavila A. Molecular basis of endothelial cell morphogenesis in three-dimensional extracellular matrices. *Anat Rec*. 2002;268:252–275. doi: 10.1002/ar.10159.
41. Carmeliet P. Angiogenesis in life, disease and medicine. *Nature*. 2005;438:932–936. doi: 10.1038/nature04478.
42. von Tell D, Armulik A, Betsholtz C. Pericytes and vascular stability. *Exp Cell Res*. 2006;312:623–629. doi: 10.1016/j.yexcr.2005.10.019.
43. Herbert SP, Stainier DY. Molecular control of endothelial cell behaviour during blood vessel morphogenesis. *Nat Rev Mol Cell Biol*. 2011;12:551–564. doi: 10.1038/nrm3176.
44. Ferguson JE I, Kelley RW, Patterson C. Mechanisms of endothelial differentiation in embryonic vasculogenesis. *Arterioscler Thromb Vasc Biol*. 2005;25:2246–2254. doi: 10.1161/01.ATV.0000183609.55154.44.
45. Armulik A, Abramsson A, Betsholtz C. Endothelial/pericyte interactions. *Circ Res*. 2005;97:512–523. doi: 10.1161/01.RES.0000182903.16652.d7.
46. Akao Y, Nakagawa Y, Kitade Y, Kinoshita T, Naoe T. Downregulation of microRNAs-143 and -145 in B-cell malignancies. *Cancer Sci*. 2007;98:1914–1920. doi: 10.1111/j.1349-7006.2007.00618.x.
47. Iorio MV, Ferracin M, Liu CG, et al. MicroRNA gene expression deregulation in human breast cancer. *Cancer Res*. 2005;65:7065–7070. doi: 10.1158/0008-5472.CAN-05-1783.
48. Michael MZ, O' Connor SM, van Holst Pellekaan NG, Young GP, James RJ. Reduced accumulation of specific microRNAs in colorectal neoplasia. *Mol Cancer Res*. 2003;1:882–891.
49. Carmeliet P, Jain RK. Angiogenesis in cancer and other diseases. *Nature*. 2000;407:249–257. doi: 10.1038/35025220.
50. Raza A, Franklin MJ, Dudek AZ. Pericytes and vessel maturation during tumor angiogenesis and metastasis. *Am J Hematol*. 2010;85:593–598. doi: 10.1002/ajh.21745.
51. Goel S, Duda DG, Xu L, Munn LL, Boucher Y, Fukumura D, Jain RK. Normalization of the vasculature for treatment of cancer and other diseases. *Physiol Rev*. 2011;91:1071–1121. doi: 10.1152/physrev.00038.2010.
52. Jain RK, Booth MF. What brings pericytes to tumor vessels? *J Clin Invest*. 2003;112:1134–1136. doi: 10.1172/JCI20087.
53. Rustom A, Saffrich R, Markovic I, Walther P, Gerdes HH. Nanotubular highways for intercellular organelle transport. *Science*. 2004;303:1007–1010. doi: 10.1126/science.1093133.
54. Jiang S, Zhang LF, Zhang HW, Hu S, Lu MH, Liang S, Li B, Li Y, Li D, Wang ED, Liu MF. A novel miR-155/miR-143 cascade controls glycolysis by regulating hexokinase 2 in breast cancer cells. *EMBO J*. 2012;31:1985–1998. doi: 10.1038/emboj.2012.45.
55. Lee SK, Teng Y, Wong HK, Ng TK, Huang L, Lei P, Choy KW, Liu Y, Zhang M, Lam DS, Yam GH, Pang CP. MicroRNA-145 regulates human corneal epithelial differentiation. *PLoS One*. 2011;6:e21249. doi: 10.1371/journal.pone.0021249.
56. Ruoslahti E. Specialization of tumour vasculature. *Nat Rev Cancer*. 2002;2:83–90. doi: 10.1038/nrc724.

57. Cho H, Kozasa T, Bondjers C, Betsholtz C, Kehrl JH. Pericyte-specific expression of Rgs5: implications for PDGF and EDG receptor signaling during vascular maturation. *FASEB J*. 2003;17:440–442. doi: 10.1096/fj.02-0340fje.
58. Yancopoulos GD, Davis S, Gale NW, Rudge JS, Wiegand SJ, Holash J. Vascular-specific growth factors and blood vessel formation. *Nature*. 2000;407:242–248. doi: 10.1038/35025215.
59. Hellström M, Gerhardt H, Kalén M, Li X, Eriksson U, Wolburg H, Betsholtz C. Lack of pericytes leads to endothelial hyperplasia and abnormal vascular morphogenesis. *J Cell Biol*. 2001;153:543–553.
60. Goumans MJ, Valdimarsdottir G, Itoh S, Rosendahl A, Sideras P, ten Dijke P. Balancing the activation state of the endothelium via two distinct TGF-beta type I receptors. *EMBO J*. 2002;21:1743–1753. doi: 10.1093/emboj/21.7.1743.

Novelty and Significance

What Is Known?

- MiR-143/145 cluster regulates smooth muscle cell (SMC) physiology and vascular homeostasis.
- Transforming growth factor β modulates SMC differentiation toward a contractile phenotype.
- MiR-143/145 can be transcribed by endothelial cells (ECs) in response to an altered laminar shear stress.

What New Information Does This Article Contribute?

- Transforming growth factor β signaling triggers miR-143/145 transfer from SMCs to ECs.
- MicroRNA transfer may take place through thin membrane structures called tunneling nanotubes although definitive proof remains to be shown.
- On endothelial uptake miR-143/145 modulate angiogenic capabilities, favoring vessel stabilization.

In this study, we demonstrate that miR-143 and miR-145 function as signaling molecules between SMCs and ECs. MiRNA passage is triggered by direct cell-to-cell contact and is modulated by the transforming growth factor β pathway. Our results suggest that both miRNAs may travel through tunneling nanotubes. Once in ECs, both miRNAs modulate gene expression leading to reduced proliferative and angiogenic properties. Once modulated by miRNAs, the EC phenotype, through a direct interaction with SMCs, leads to better vessel stabilization. These results provide new insights on the role of these miRNAs in neoangiogenesis.

SUPPLEMENTAL MATERIAL

TGFβ triggers miR-143/145 transfer from smooth muscle cells to endothelial cells, thereby modulating vessel stabilization.

Short Title: Climent, miR143/145 modulates EC biology

Montserrat Climent, MSc, Manuela Quintavalle, PhD, Michele Miragoli, PhD, Ju Chen, PhD, Gianluigi Condorelli, MD, PhD and Leonardo Elia, PhD

Detailed Methods

Animals

All mouse procedures on mice were performed according to institutional guidelines in compliance with national (4D.L. N.116, G.U., suppl. 40, 18-2-1992) and international law and policies (EEC Council-Directive 86/609, OJ L 358,1,12-12-1987; NIH Guide for the Care and Use of Laboratory Animals, US National Research Council-1996 and new directive 2010/63/EU). 8 weeks old C57/b6 mice were used for the experiments. Special attention was paid to animal welfare and to minimize the number of animals used and their suffering. Myh11-cre/ERT2[1] were kindly donated by Prof. Stefan Offermanns (Max-Planck-Institute for Heart and Lung, Bad Nauheim) and crossed with miR-143/145 floxed mice. Gene knock-down was induced by i.p. tamoxifen (Sigma) injection for 5 consecutive days at the concentration of 50mg/kg.

Pressure over-load was induced by trans-aortic constriction as described before.[2] *In vivo* matrigel plug assays were carried out using Geltrex® Matrix (Life Technologies) as previously described.[3]

Cell culture

Human umbilical vein endothelial cells (HUVECs) were purchased from Life Technologies and grown in M200 (Life Technologies) with supplementary growth factors LSGS (Life Technologies). Mouse endothelial cells (H5V), kindly donated by Dr. A. Vecchi (Humanitas), were cultured in DMEM (Lonza) supplemented with 10% FBS (Lonza), 2 mM glutamine, 1 mM sodium pyruvate, and 100 U/ml penicillin-streptomycin. ove. HUVECs from passages 3–8 were used for the experiments. For virus production, HEK-293T cells were cultured in DMEM with 10% FBS as above. All cultures were maintained in a humidified 5% CO_2 atmosphere at 37º C. For all co-cultures, $2x10^4$ ECs and $2x10^4$ SMCs were seeded for 24 h in M200 or DMEM 10% FBS. For transwell assays, PET membranes with 1.0 µm pore size were used (Millipore). For no-contact transwell assays, SMCs were first plated in 12-well plates, then transwells were inserted in the wells and ECs were seeded on top. For contact transwell assays, SMCs were first plated on the bottom site of the transwell for 2 h at 37ºC to let them attach, and subsequently transwells were transferred into the wells of a 12-well plate and ECs seeded on top. For treatments, cells were washed with PBS, serum-starved for 24 h, and then treated with 10 ng/ml TGFβ (Peprotech), PDGF (Sigma), FGF, TNFα, or EGF (Peprotech). The TGFβ inhibitor SB431542 (Sigma) was used at a concentration of 10 µM. Latrunculin A (LatA) (Sigma) was added at the final concentration of 0.5 µM. For conditioned media assay, medium was collected after 24 h of culture and added to the selected cells. Exosome inhibitors were used at the following concentrations: GW4869 (2 µM) , NH_4Cl (200 µM), and chloroquine (0.4 µM).

Smooth muscle cells expressing CD63-GFP and treatments

For the study of exosomes, lentiviral particles encoding CD63-GFP (Lenti-CD63-GFP) were purchased from SBI and used to transduce SMCs. CD63-GFP-SMCs were used to study the secretion of CD63-vesicles using different stimuli (PDGF, FGF, TGFβ). After treatments,

conditioned medium containing the CD63-GFP vesicles were either used to evaluate the fluorescence in the medium or added to ECs in order to detect the uptake of these vesicles. Exosomes were purified with ExoQUICK solution (SBI) following manufacturer's instructions.

Ago2 immunoprecipitation

ECs transfected with 50nM of the control, miR-143, or miR-145 mimics (Dharmacon) were washed with 1xPBS and UV-crosslinked for 30 sec at 400 mJ. Afterwards, cells were harvested and washed twice with 1xPBS. Cell pellets were resuspended and incubated 5 min on ice in 700 µl of lysis buffer (150 mM KCl, 25 mM Tris pH 7.4, 5 mM EDTA, 0.5% NP-40, 5 mM DTT) supplemented with protease inhibitor cocktail (Roche) and 100 U/ml RNase inhibitor (Life Technologies). Thereafter, lysates were centrifuged for 10 min at 10,000 g and cytoplasmic lysates recovered. Magnetic beads were washed and pre-blocked in PBS with 0.5% BSA and then anti-Ago2 (Ascension) was added and incubated 1 h at 4º C with rotation. 10% of the cytoplasmic lysate was kept as input and the rest was incubated with the Ago2-beads O/N at 4ºC in rotation. Tubes were then placed in the magnet, and beads washed three times. Finally, 1 ml of Purezol (BioRad) was added to the samples for RNA extraction.

Luciferase reporter assay

HKII-3´-UTR and ITGβ8-3′-UTR plasmids were co-transfected with the miR-143 or miR-145 mimics (Dharmacon) and relative controls, using lipofectamine 2000 (Life Technologies). 3′UTR site-specific mutagenesis at the predicted sites for each target was performed using the QuikChange Site-Directed Mutagenesis Kit, as described by the manufacturer (Stratagene). Cells were harvested 48 h after transfection and analyzed with the dual-luciferase reporter assay kit (Promega), according to manufacturer's protocol.

RNA extraction and qRT-PCR

Total RNA was isolated using Purezol reagent (BioRad) according to manufacturer's protocol. For gene expression, RNA was reverse transcribed with High capacity cDNA archive kit (Applied Biosystems) and qRT-PCR was performed using Select SYBR Green (Applied Biosystems). PCR primers are listed in Table I. For miRNA expression, RNA was reverse transcribed using the miRCURY LNA™ Universal RT (Exiqon). SYBR Green was used to perform the quantitative real-time PCR for mature miR-143, miR-145, miR-15, and miR-16 (Exiqon), and U6, as internal control. For exosome quantification we used a spike-in miRNA (Exiqon) as internal control as previously described.[4]

Western blot

Cells were lysed in RIPA buffer and sonicated for 5 cycles (30 sec on, 30 sec off) using a Biorupture™ Next Gen (Diagenode). After quantification using DC™ Protein Assay (BioRad), the same quantity of protein was separated in 4–12% NuPAGE® Bis-Tris precast gel (Life Technologies) and transferred to a nitrocellulose membrane (Biorad). Afterwards, anti-HKII (Santa Cruz Biotechnologies), anti-ITGβ8 (Santa Cruz Biotechnologies), and anti-GAPDH (Santa Cruz Biotechnologies) were incubated overnight at 4ºC, and secondary peroxidase-conjugated antibodies incubated for 1 h at room temperature. Immobilon Western Chemiluminiscent HRP (Millipore) was used for protein visualization using a ChemiDoc (BioRad). Bands were quantified using ImageJ software and results are expressed relative to the control.

Cell transfection

Primary mouse SMCs: cells were plated in 6-well plate at $1x10^5$ cells/well. For oligo miR-143 and -145 mimics conjugated with Alexa-488 (IDT), cells were transfected at the concentration of 100 nM using Lipofectamine LTX (Invitrogen). For Cx43 and TGFβR2 knockdown, pLKO-shCx43 and –TGFβR2 were used (Respectively: Sigma #TRCN0000068477 and

#TRCN0000294529) with the corresponding control pLKO-shScr (Sigma # SHC002). Primary murine SMCs with stable expression of the shCx43 and shTGFβR2 were generated using a virus MOI of 5 together with 5 μg/ml of polybrene (Sigma).
HUVECs: cells were plated in 12-well plates at $3x10^4$ cells/well. For anti-miR experiments, cells were transfected with anti-miR-143 and -145 or control scrambled oligonucleotides (Exiqon) at 100 nM using Lipofectamine RNAiMAX (Life Technologies). For siRNA experiments, cells were transfected with specific siRNA against ITGβ8 (IDT # HSC.RNAI.N000002214.12.1) at 80 nM using Lipofectamine RNAiMAX (Life Technologies). On the other hand, knockdown of HKII was obtained infecting the cells with lentiviral particles expressing the specific shRNAs (Sigma # TRCN0000037671).

Scanning electron microscopy
Cells were fixed with 2.5% glutaraldehyde in 0.1 M tampon cacodylate (pH 7.2) for 30 min at room temperature (RT). Samples were washed with phosphate buffered saline (PBS) at RT and dehydrated through a series of different concentration of alcohols. The samples were covered with few nanometers of gold with a coating device. The cell structure and topography were observed with a scanning electron microscope (SEM) Supra™ 40 (Zeiss, DE) equipped with InLens detector and operated with an acceleration of 3 kV.

Generation of lentiviral vectors harboring miRNAs and decoys
For gain- and loss-of-function of miR-143 and miR-145 in ECs, production of Lenti-Empty (CTR), Lenti-miR-143, Lenti-miR-145, Lenti-Decoy-miR-143, and Lenti-Decoy-miR-145 was performed as previously described.[5]

Co-culture with the decoy system
ECs (H5V) were transduced with Lenti-Decoy-miR-143 and -145. $5x10^3$ cells were plated in a 12-well plate together with $20x10^3$ WT or miR-143/145-KO SMCs on coverslips. After 72 h of co-culture, cells were fixed and stained for F-actin with Phalloidin-Alexa-594 (Life Technologies).

***In situ* hybridization**
In situ hybridization was performed with microRNA ISH Optimization Kit (Exiqon), following the manufacturer's indications.

Proliferation assay
ECs were plated at $1x10^4$ cells/well in 6-wells plates. After 24 h, cells were transduced or transfected with the respective lentiviral particles or siRNA. Cell proliferation was determined at 48, 72, and 96 hours after transduction/transfection.

BrdU incorporation assay
EC cultures were treated with BrdU (Life Technologies) for 24 h, following the manufacturer's protocol. Then, cells were fixed with 4% paraformaldehyde and permeabilized with PBS/1% Trition-X100, treated with HCl, and stained with anti-BrdU antibody (Santa Cruz Biotechnology).

Immunofluorescence
To determine the formation of the TNTs and characterize the proteins involved in their formation during ECs/SMCs co-cultures, the following reagents were used: anti-lectin-FITC (BS-1 from Sigma), anti-αSMA (Sigma), anti-Cx43 (Sigma), anti-tubulin (Cell Signaling), anti-Cdc42 (Cell Signaling), Phalloidin-Alexa-594 or -647 (Life Technologies).

Confocal analysis
Confocal images were obtained with a microscope (IX81-FV1000; Olympus) using FluoView software (Olympus) at room temperature.

Live imaging
The experiments were performed plating HUVECs and primary SMCs on glass plates at the ratio 1:1. SMCs were transfected with oligo miR-143-Alexa-488 or miR-145-Alexa-488 24 h before the imaging, while HUVECs were labeled with CellTracker™ Red CMTPX Dye (Life Technologies) following manufacturer's protocol. Once in co-culture, pictures were taken every 3 minutes using the CellR system (Olympus) with a 40X objective in a humidified 5% CO_2 atmosphere at 37º C. Video reconstructions were realized using Fiji software.

Flow Cytometry analysis
Evaluation of the EC purity after Pecam1-beads separation was performed with intra-cellular staining of both EC and SMC fractions using an αSMA-FITC antibody (Sigma). Measurements were obtained with a FACS Canto II instrument (BD Bioscience).

Tube formation assay
Plates pre-coated with Geltrex® Matrix (Life Technologies) were used. EC tube formation assay was performed seeding the ECs at $1x10^4$ cells/well into 96-well plates or in 48-well plate for the co-culture seeding $6x10^4$ HUVEC and $3x10^4$ SMCs per well. The degree of tube formation was evaluated using an inverted microscope after 24 h incubation at 37ºC and 5% CO_2.

Enzyme-linked immunosorbent assay (ELISA)
Conditioned media were collected for measuring the presence of different secreted proteins: VEGF, TNFα, IL-10, IL-6, and TGFβ1 (R&D Systems). Samples were diluted so that the optical density fell within the optimal portion of a log standard curve. TGFβ1 was assayed on acid-activated samples, following the manufacturer's protocol.

Supplemental Figures and Figure Legends

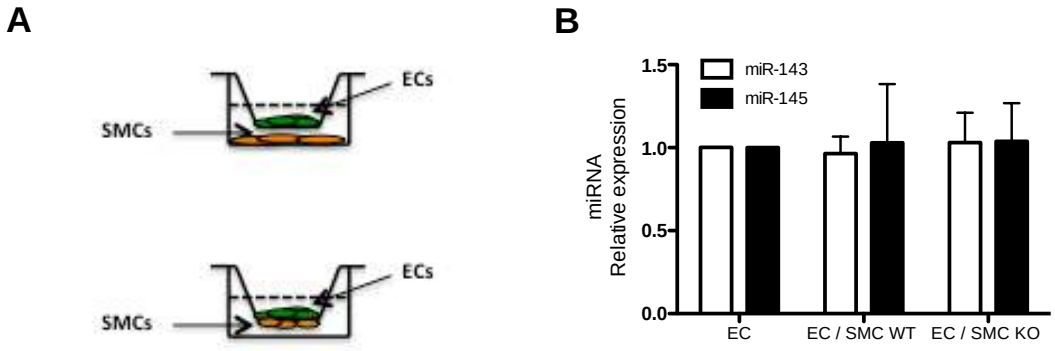

Online Figure I

Online Figure I. EC/SMC co-culture with no physical contact. (A) Cartoon illustrating how co-culture experiments were performed. (B) Mature miR-143 and miR-145 were measured on ECs (HUVEC) after 24 h of no-contact co-culture with WT and miR-143/5 KO SMCs. Data for B are plotted and analyzed as described in Figure 1.

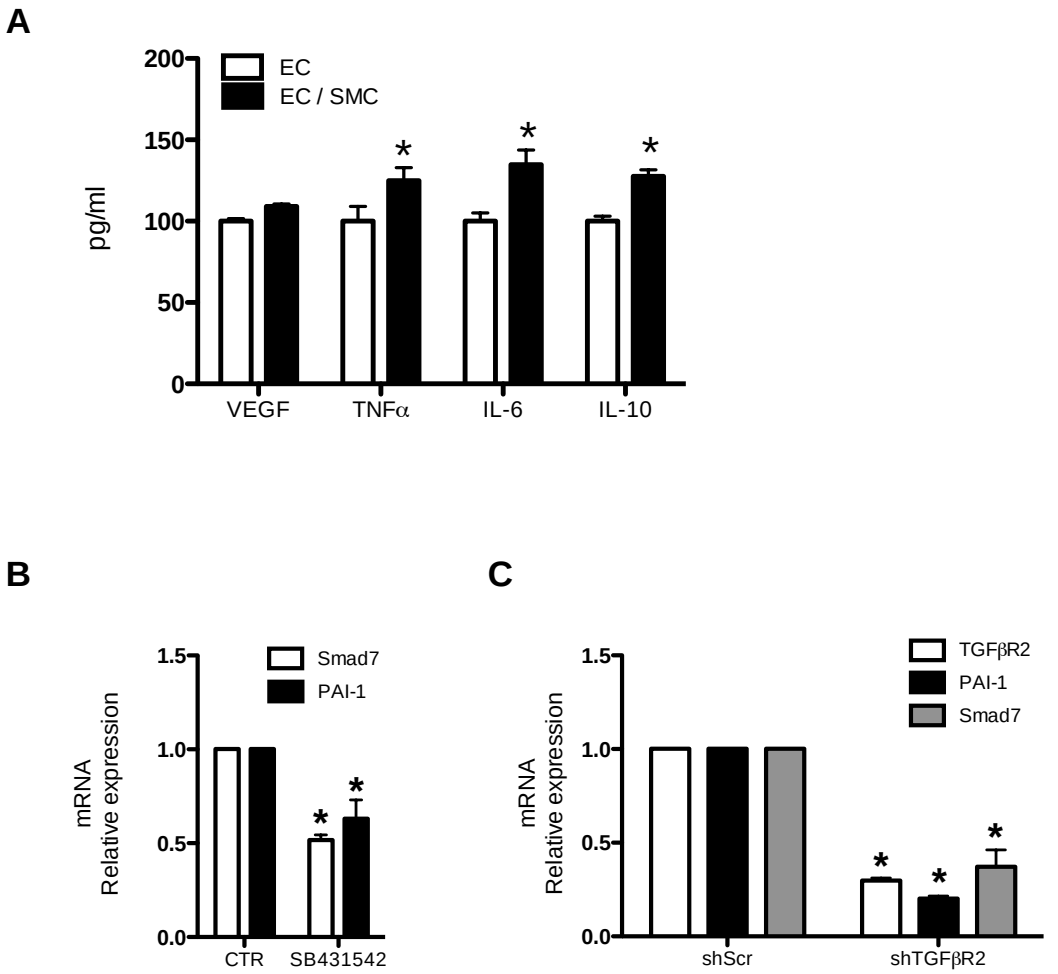

Online Figure II

Online Figure II. Cytokines secreted by ECs in co-culture with SMCs. (A) Medium from the EC/SMC co-culture was collected after 24 h and the levels of hVEGF, hTNFα, hIL-6, and hIL-10 measured by ELISA. (B) TGFβ readout genes (PAI-1 and Smad7) were measured in SMCs CTR or treated with the TGFβ inhibitor SB431542 after co-culture. (C) TGFβR2, PAI-1 and Smad7 RNA levels in SMCs transduced with a shRNA against TGFβR2 after co-culture. *, $P<0.05$. Data are plotted and analyzed as described in Figure 2.

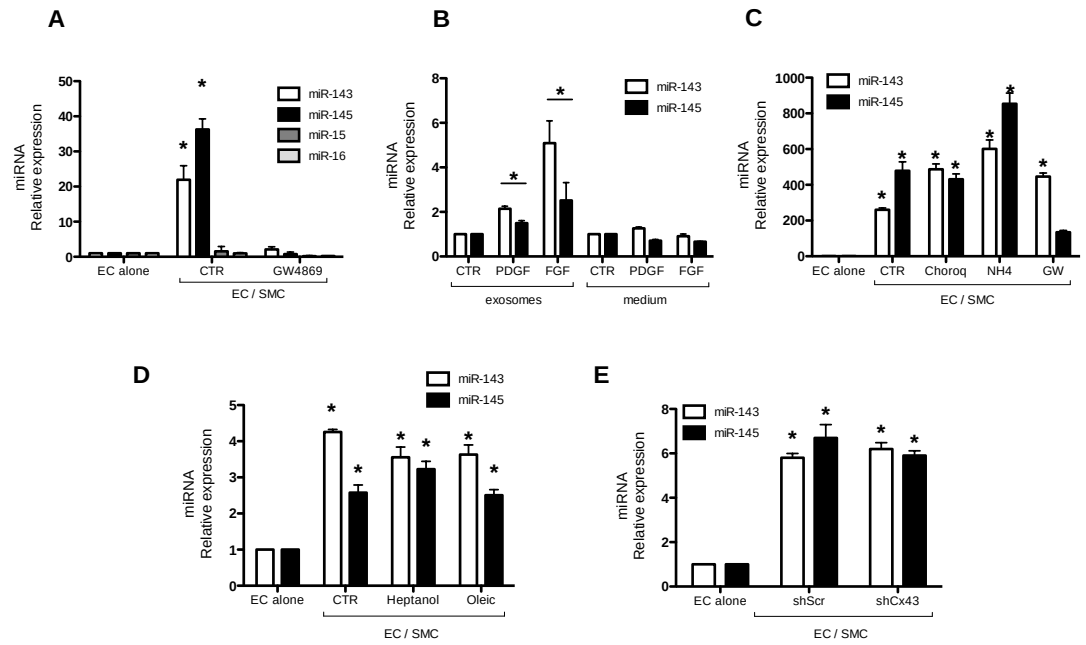

Online Figure III

Online Figure III. miR-143 and miR-145 secretion and transfer inhibition by specific agents. (A) MiR-143, - 145, -15, and -16 were measured in exosomes from EC/SMC co-culture treated or not with the exosome inhibitor GW4869. (B) MiR-143 and -145 were analyzed in exosomes of SMCs treated with PDGF or FGF and in the relative conditioned medium. (C) MiR-143 and -145 were measured in ECs (HUVEC) after co-culture with WT SMCs treated or not with different exosomes inhibitors (Chloroq: chloroquine; NH4: NH_4Cl ; GW: GW4869). (D) MiR-143 and -145 were measured in EC/SMC co-cultures after treatment with gap junction uncoupler agents (heptanol and oleic acid). (E) MiR-143 and -145 were measured in EC/SMC co-cultures transduced with a lentivirual vectors expressing shRNA against Cx43. *, P<0.05. Data are plotted and analyzed as described in Figure 1.

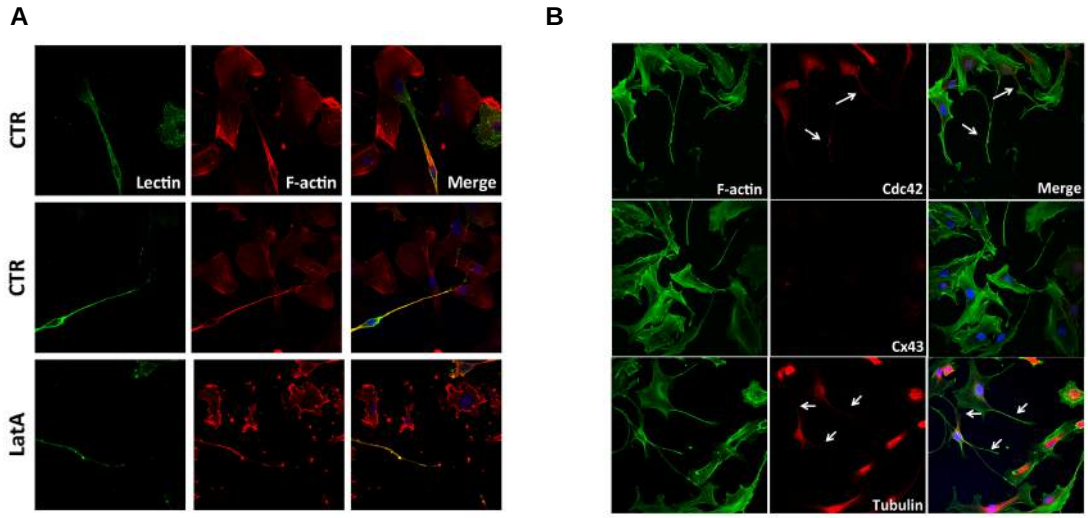

Online Figure IV

Online Figure IV. Characterization of tunneling nanotubes. (A) Lectin-FITC and Phalloidin-Alexa-594 staining on EC/SMC co-culture following LatA treatment. White arrows indicate TNTs (Magnification: 40x); (B) F-actin together with Cdc42 or Cx43 or Tubulin (Magnification: 40x).

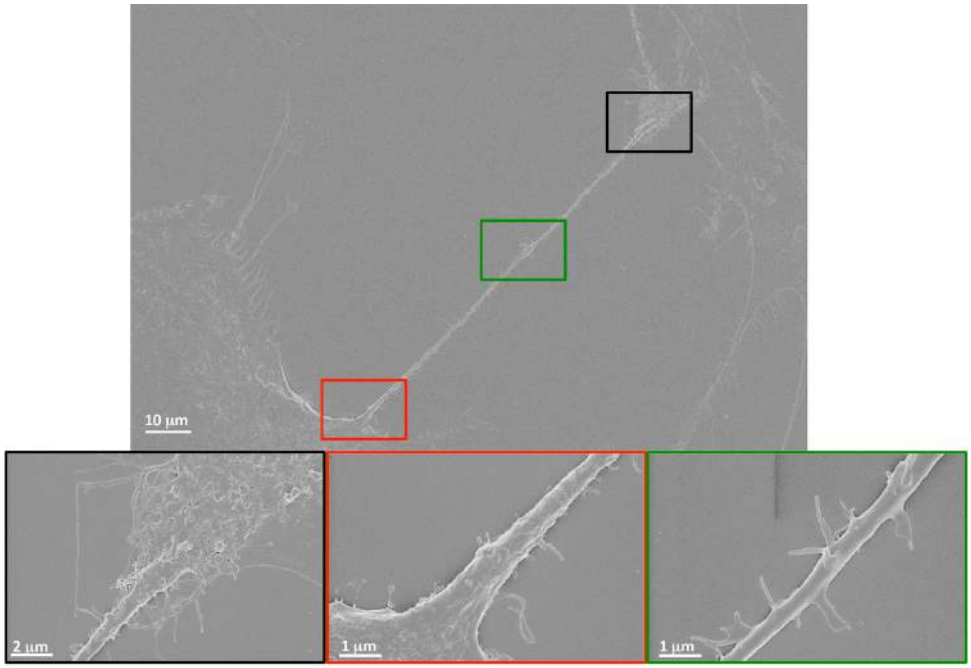

Online Figure V

Online Figure V. TNT characterization by scanning electron microscopy (SEM). Representative image of a TNT formed between an SMC and an EC.

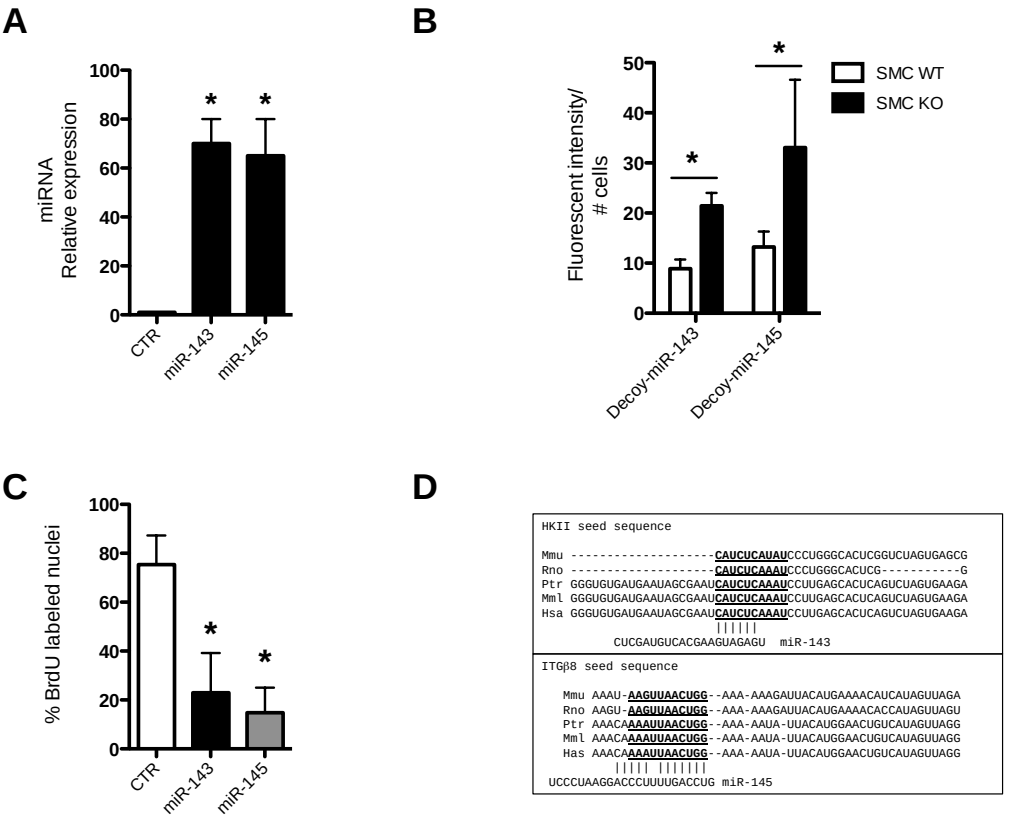

Online Figure VI

Online Figure VI. miR-143 and -145 activity on ECs. (A) MiR-143 and -145 levels in over-expressing ECs. (B) Quantification of GFP signal for decoy experiments shown in Figure 4D. (C) Quantification of BrdU staining shown in Figure 4G. (D) Conservation of *HKII* and *ITGβ8* seed sequences in different species. (E) BrdU staining in ECs (HUVEC) transduced with SCR (scrambled) sequence or siRNAs vs HKII and ITGβ8 (magnification: 20x).

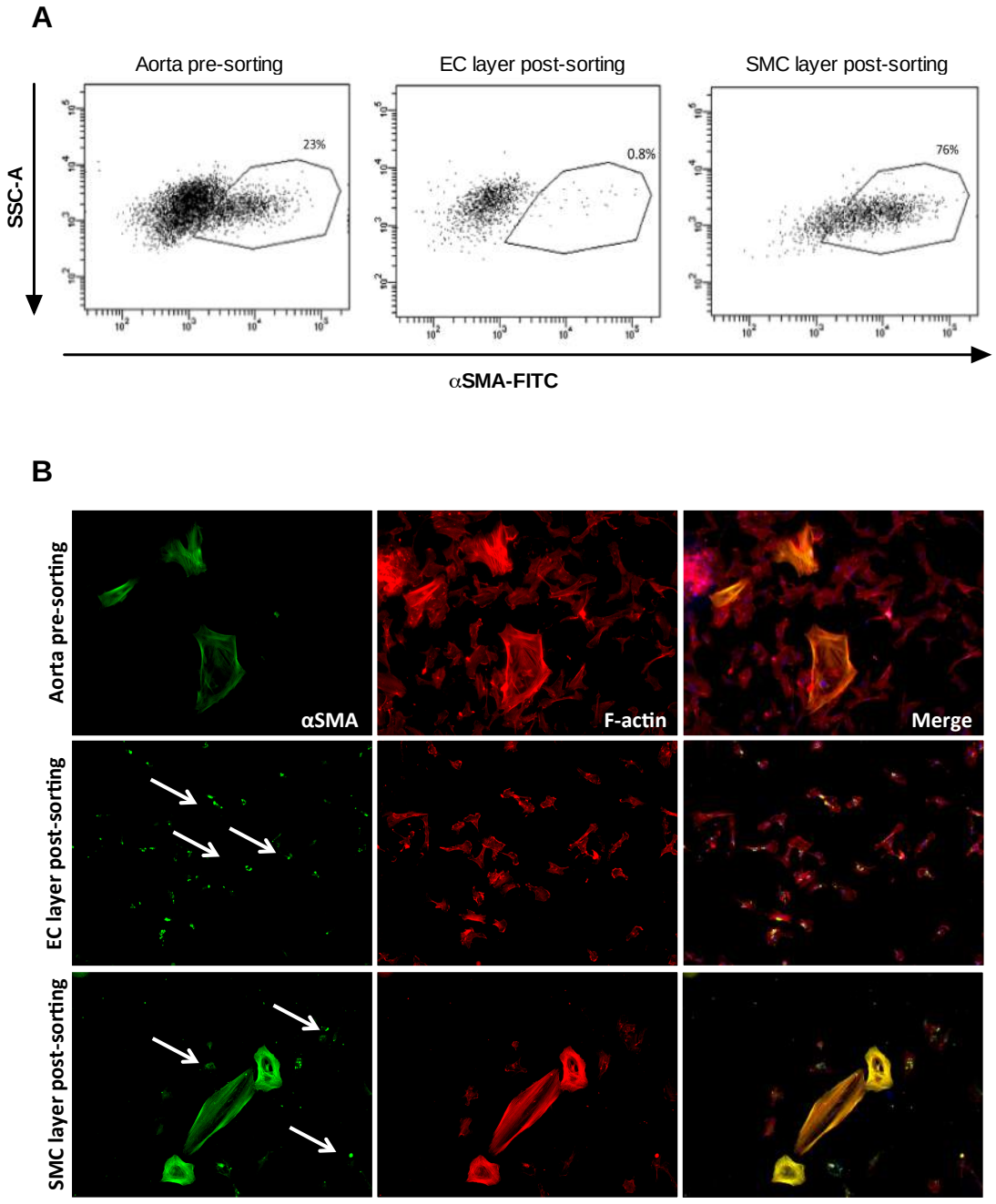

Online Figure VII

Online Figure VII. Evaluation of EC purity following separation with Pecam1 beads. (A) EC and SMC layers from aorta were separated using Pecam1 beads. After separation, intracellular staining was performed on EC and SMC fractions using an αSMA-FITC conjugated antibody; (B) Immunofluorescence of EC and SMC fractions following separation with anti-Pecam1 beads. White arrows indicate auto-fluorescence of magnetic beads.

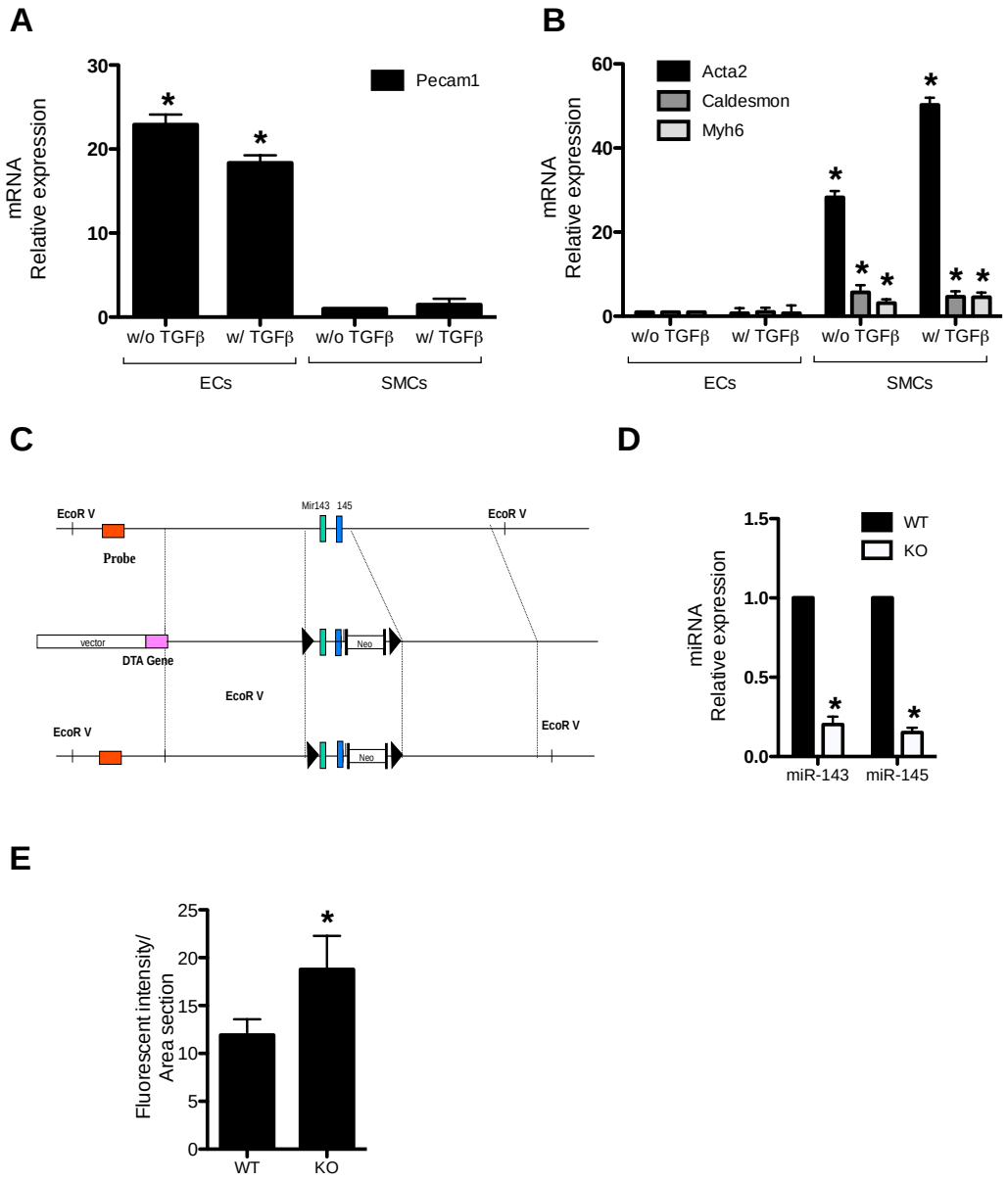

Online Figure VIII

Online Figure VIII. Inducible miR-143/145 SMC-specific knockout mouse. (A and B) Levels of *Pecam1* and *Acta2* mRNAs in EC and SMC fractions after cell isolation were analyzed with qRT-PCR. (C) Strategy design for mouse generation. (D) MiR-143 and -145 levels on aortas of WT (cre+) and KO (floxed/cre+) mice upon tamoxifen induction. (E) Quantification of the plug matrigel assay reported in Figure 6F.

Supplemental Table

Supplementary table I. Primers used in this study

Primers		
Gene*	**Forward**	**Reverse**
mpri-miR-143	CCTCCTGCCCAAGAAGAAAG	TCTCAGACTCCCAACTGACCA
mpri-miR-145	CTTTCCAAGCCACTCAAAGC	GCGCTGTATACACCCTCCTT
hpri-miR-143	CCCTCTAACACCCCTTCTCC	TCTCAGACTCCCAACTGACCA
hpri-miR-145	CCAGAGGGTTTCCGGTACTT	CGGATGTGGCTTATTGCTCT
mActa2	CTGACAGAGGCACCACTGAA	CATCTCCAGAGTCCAGCACA
mCalponin	GGCAGGAACATCATTGGACT	GACCTGGCTCAAAGATCTGC
mCaldesmon	GGAGGCTGTGCTGATGGTAT	TCTGTCCTGCTCAGCTTTGA
mMhy6	AACAGGTGATGGCAAGATCC	GCAGGAAGTGCTCAAAGTCC
mTGFβR2	AAGCCTCCAGACTTCCCATT	ACTTTTGTCGTGGGTTCTGG
mSmad7	TTCTCAAACCAACTGCAGGC	GTTGGGAATCTGAAAGCCCC
mPAI-1	TACACTGAGTTCACCACCCC	CGATGAACATGCTGAGGGTG
heNOS	CCCTTCAGTGGCTGGTACAT	TATCCAGGTCCATGCAGACA
hTie-2	ACAATGGTGTCTGCCATGAA	TTCACAAGCCTTCTCACACG
hIL-8	GTGCAGTTTTGCCAAGGAGT	AAATTTGGGGTGGAAAGGTT
hCTGF	GCACAAGGGCCTATTCTGTC	ACGTGCACTGGTACTTGCAG
hMMP2	TGACATCAAGGGCATTTCAGGAGC	GTCCGCCAAATGAACCGGTCCTTG
hFGF1	AAGGGGAAATCACCACCTTC	CCCCGTTGCTACAGTAGAGG
hFGF2	AGCGGCTGTACTGCAAAAAC	CTTGATGTGAGGGTCGCTCT
hANG2	GCAAGTGCTGGAGAACATCA	CACAGCCGTCTGGTTCTGTA
hCXCL12	AGAGCCAACGTCAAGCATCT	CTTTAGCTTCGGGTCAATGC
hFLK1	TGATCGGAAATGACACTGGA	CACGACTCCATGTTGGTCAC
hTGFβ1	GTGGAAACCCACAACGAAAT	CGGAGCTCTGATGTGTTGAA
hPecam1	AGGTGTTGGTGGAAGGAGTG	ACAGTTGACCCTCACGATCC
hHKII	AAGGGCAGAAGGGGAAGATA	AGCCAATTGCTGTGGTCTCT
hITGβ8	CACCATGGAAATCTGTGTGC	ACACTTGGCCCTTTGAATTG
U6	CGCTTCGGCAGCACATATAC	TTCACGAATTTGCGTGTCAT

*m=mouse; h=human

Supplemental References

1. Wirth A, Benyo Z, Lukasova M, Leutgeb B, Wettschureck N, Gorbey S, Orsy P, Horvath B, Maser-Gluth C, Greiner E, Lemmer B, Schutz G, Gutkind JS and Offermanns S. G12-G13-LARG-mediated signaling in vascular smooth muscle is required for salt-induced hypertension. *Nat Med*. 2008;14:64-8.
2. Rockman HA, Ross RS, Harris AN, Knowlton KU, Steinhelper ME, Field LJ, Ross J, Jr. and Chien KR. Segregation of atrial-specific and inducible expression of an atrial natriuretic factor transgene in an in vivo murine model of cardiac hypertrophy. *Proc Natl Acad Sci U S A*. 1991;88:8277-81.
3. Wang S, Aurora AB, Johnson BA, Qi X, McAnally J, Hill JA, Richardson JA, Bassel-Duby R and Olson EN. The endothelial-specific microRNA miR-126 governs vascular integrity and angiogenesis. *Developmental cell*. 2008;15:261-71.
4. Fichtlscherer S, De Rosa S, Fox H, Schwietz T, Fischer A, Liebetrau C, Weber M, Hamm CW, Roxe T, Muller-Ardogan M, Bonauer A, Zeiher AM and Dimmeler S. Circulating microRNAs in patients with coronary artery disease. *Circ Res*. 2010;107:677-84.
5. Bonci D, Coppola V, Musumeci M, Addario A, Giuffrida R, Memeo L, D'Urso L, Pagliuca A, Biffoni M, Labbaye C, Bartucci M, Muto G, Peschle C and De Maria R. The miR-15a-miR-16-1 cluster controls prostate cancer by targeting multiple oncogenic activities. *Nat Med*. 2008;14:1271-7.

Video Legends

Online Video I. Co-culture of primary SMCs transfected with miR-143-Alexa 488 and ECs (HUVEC) pre-labeled with CellTracker™ Red CMTPX Dye (Life Technologies).

Online Video II. Co-culture of primary SMCs transfected with miR-145-Alexa 488 and ECs (HUVEC) pre-labeled with CellTracker™ Red CMTPX Dye (Life Technologies).

Circulation Research
JOURNAL OF THE AMERICAN HEART ASSOCIATION

TGFβ Triggers miR-143/145 Transfer From Smooth Muscle Cells to Endothelial Cells, Thereby Modulating Vessel Stabilization

Montserrat Climent, Manuela Quintavalle, Michele Miragoli, Ju Chen, Gianluigi Condorelli and Leonardo Elia

Circ Res. 2015;116:1753-1764; originally published online March 23, 2015;
doi: 10.1161/CIRCRESAHA.116.305178
Circulation Research is published by the American Heart Association, 7272 Greenville Avenue, Dallas, TX 75231

Print ISSN: 0009-7330. Online ISSN: 1524-4571